Frequency synchronization for OFDM-Based Massive MIMO systems

Article *in* IEEE Transactions on Signal Processing · April 2019

DOI: 10.1109/TSP.2019.2911249

CITATION
1

READS
245

4 authors:

Parna Sabeti
Trinity College Dublin
7 PUBLICATIONS **7** CITATIONS
SEE PROFILE

Arman Farhang
National University of Ireland, Maynooth
81 PUBLICATIONS **986** CITATIONS
SEE PROFILE

Nicola Marchetti
Trinity College Dublin
208 PUBLICATIONS **1,694** CITATIONS
SEE PROFILE

Linda Doyle
Trinity College Dublin
252 PUBLICATIONS **3,821** CITATIONS
SEE PROFILE

Frequency Synchronization for OFDM-based Massive MIMO Systems

Parna Sabeti, Arman Farhang, Nicola Marchetti, and Linda Doyle

***Abstract*—Massive multiple input multiple output (MIMO) is a key technology in the fifth generation (5G) wireless networks. However, its performance heavily relies on accurate synchronization. Additionally, synchronization can impose an enormous amount of computational complexity to the system. To deal with this issue, in this paper, we propose a low complexity frequency synchronization technique with a high accuracy for the uplink of multi-user orthogonal frequency division multiplexing (OFDM) based massive MIMO systems. First, we propose a carrier frequency offset (CFO) estimation whose computational complexity increases only linearly with respect to the number of base station (BS) antennas. Second, we propose a CFO compensation method that is performed after combining the received signals at the BS antennas, and as a result, its computational complexity is independent of the number of BS antennas. As a third contribution, the effect of the CFO estimation error is studied, and it is proven that by applying our proposed CFO compensation technique, the CFO estimation error causes only a constant phase shift. We then propose an algorithm to efficiently calculate and remove the estimation error. Our simulation results testify the efficacy of our proposed synchronization technique. As it is demonstrated, our proposed synchronization technique leads to a bit error rate (BER) performance that is very close to the one for a fully synchronous system.**

I. Introduction

Large scale multiple input multiple output (MIMO) or massive MIMO is one of the key technologies for the fifth generation (5G) wireless networks, [2], [3]. The main difference between massive MIMO and classical multi-user MIMO systems is the large number of antennas at each base station (BS) which brings significant advantages to these systems. It can tremendously enhance network capacity by enabling users to simultaneously utilize the entire available bandwidth even in presence of pilot contamination [4]–[6]. This leads to an improved spectral efficiency [7]. In addition, by increasing the number of BS antennas (array gain), the required power to achieve a desired information rate can be reduced [7]. Moreover, large-scale antenna arrays are crucial for achieving highly directional beamforming. Hence, emergence of millimeter wave (mmWave) systems, where beamforming plays a vital role, has further highlighted the importance of massive MIMO, [8].

All the above advantages of massive MIMO systems rely on accurate synchronization. However, massive MIMO systems heavily suffer from synchronization errors, such as, timing offset (TO) and carrier frequency offset (CFO), [9], [10], [11]. In orthogonal frequency division multiplexing (OFDM), the effects of TO can be absorbed into the cyclic prefix (CP) provided that an adequately long CP is utilized, [12]. However, frequency synchronization is still a challenging problem. Although, there exists a substantial amount of work reported on the frequency synchronization for conventional multi-user OFDM systems, [13]–[15], not all of them are applicable to massive MIMO systems.

In the past decade, a number of studies have been conducted to address the synchronization problem in OFDM-based MIMO systems. The work in [16] derived a joint CFO and channel estimator based on the maximum likelihood (ML) criterion for small-scale MIMO OFDM system, whose computational complexity exponentially increases with the number of users. A sub-optimal estimation algorithm using constant amplitude zero auto-correlation (CAZAC) training sequences was proposed in [17]. Another ML-based estimator with iterative interference cancellation was proposed in [18] for coordinated multi-point (CoMP) MIMO OFDM systems. The authors in [19] developed an algorithm for joint CFO compensation and multi-user detection in small-scale multi-user MIMO systems. In another work [20], the authors proposed a pilot-based two stage CFO and phase noise (PN) compensation for point to point high frequency MIMO OFDM, where both stages use a conventional least squares (LS) method and need to calculate the inverse of a full rank matrix. In [21], authors proposed a joint ML-based CFO and channel estimation method which requires a multidimensional grid search. To solve this issue, the authors in [22] converted the ML CFO estimator into a set of line search problems. However, this algorithm still requires per antenna CFO estimation for all the users leading to a substantial amount of computational burden.

To reduce the complexity of frequency synchronization for massive MIMO systems, some works combine the received signals at all the BS antennas and extract the users' CFOs from the resulting signal. The authors in [23] proposed a joint spatial-frequency alignment technique in which users' pilots can be distinguished using their estimated angles of arrival. However, when the users are not spatially separated, their angles of arrival are very close, if not the same. As a result, the users' signals cannot be accurately distinguished from each other. In [24], an improved user grouping scheme has been designed to deal with this issue, where the CFO estimation and data detection are jointly performed for the users that are close to one another. Despite the imposed computational burden due to the multi-user interference (MUI) cancellation, this technique still cannot accurately compensate the CFO effects. In [25], the authors proposed a scattered pilot-based frequency synchronization technique which can estimate CFO for each user individually by exploiting the spatial dimensions offered

Parts of the concepts based on which the contributions of this paper are built have been presented in [1].

P. Sabeti, N. Marchetti, and L. Doyle are with CONNECT, The Telecommunications Research Centre, Trinity College Dublin, Ireland, (e-mail: {sabetip, nicola.marchetti , ledoyle}@tcd.ie).

A. Farhang is with CONNECT, Maynooth University, Ireland, (e-mail: arman.farhang@mu.ie).

by the large number of BS antennas. The authors also designed a beamforming matrix for MUI cancellation. The amount of complexity of this technique is also large and goes up rapidly by increasing the number of BS antennas. In [26], the authors proposed a blind CFO estimation technique based on the covariance matrix of the received signals over all BS antennas in the frequency domain, where different null subcarriers are assigned to different users. This approach is followed by a blind MUI cancellation and channel estimation. A more computationally efficient blind CFO estimation was proposed in [27] which cancel the MUI by using the eigendecomposition of the covariance matrix of the received signals over all the BS antennas in frequency domain. After MUI cancellation, the system is like a set of parallel single user signals, and the conventional single user CFO estimation proposed in [28] is performed. In addition, an iterative CFO estimation procedure was proposed to enhance the MUI cancellation and CFO estimation accuracy in [27]. In each iteration of the algorithm proposed in [28], all received signals are taken to the frequency domain and the eigendecomposition of their covariance matrix is calculated which add a large amount of computational complexity to the system.

A low complexity CFO estimation was proposed in [29], where the authors used series of impulses for the users' pilots to provide time-domain orthogonality among different users. Hence, the received signals on each sample carry the information of only one user. Therefore, CFO of a certain user can be estimated from the combination of the received signals on the respective samples over all the BS antennas. The complexity of this approach increases only linearly with the number of BS antennas and is also independent of the number of users. However, long pilot sequences are required for an accurate estimation, especially when we need to serve many users. This technique is originally proposed for single carrier systems, while it can straightforwardly extended to multicarrier systems. The performance of this technique is studied in [30]. Since the the proposed technique in [29] suffers from high peak to average power ratio (PAPR), the spatially averaged periodogram based CFO estimation was proposed which uses a constant envelope pilot sequence to preserves users' orthogonality through different phases. This technique still needs a long pilot sequence, and also its computational complexity is higher than for our proposed technique.

To address the drawbacks of the available solutions in the literature, in this paper, we propose a frequency synchronization technique that can provide a high estimation accuracy while having a low computational complexity. This makes our proposed technique attractive for implementation of practical systems. The contributions of this paper are as follows:

- We propose a CFO estimation technique whose computational complexity increases only linearly with respect to the number of BS antennas and is independent of the number of users. We use a training sequence which is orthogonal onto the space spanned by the desired user's pilot to extract its signal from the covariance matrix of the received signals at BS antennas. Our proposed technique does not need a long pilot sequence, and one pilot symbol is sufficient. In addition, unlike the above mentioned literature, our proposed technique is not limited to the CFO range $[-0.5, 0.5]$, and can estimate both integer and fractional CFO values. It is worth to note that the local oscillator accuracy is usually in the order of parts-per-million (ppm) of the carrier frequency. Hence, it is crucial to the systems operating at high frequencies such as mmWave bands to deal with large CFO values containing both integer and fractional parts.
- We propose a CFO compensation technique that is performed after combining the received signals at the BS antennas. As a result, the compensation process is independent of the number of BS antennas. Moreover, one combiner can be used for all the users, unlike the conventional CFO compensation performed in the time domain which requires separate receivers for different users. Therefore, the computational complexity of the receiver is substantially reduced.
- We study the effect of CFO estimation error on the channel estimation and CFO compensation. We prove that by applying our CFO compensation technique, the estimation error is canceled through the compensation process and only a constant phase shift remains. Based on this result, we propose a CFO estimation error correction algorithm. As it is illustrated through simulation, mean square error (MSE) performance is improved by 3 orders of magnitude after error correction. According to the bit error rate (BER) curves in our simulations, we demonstrate that an almost perfect synchronization can be achieved.

The rest of the paper is organized as follows. The system model for the uplink of OFDM-based multi-user massive MIMO system is presented in Section II. The CFO estimation technique is proposed in Section III, and the ML channel estimation is briefly explained in Section IV. Then, in Section V, we explain our proposed CFO compensation technique. In Section VI, we study the effect of the CFO estimation error on our synchronization technique. As a result of our analysis in Section VI, in Section VII, we propose an error correction algorithm to further improve the system performance. The computational complexity of our proposed CFO synchronization technique is studied in Section VIII. Then, our proposed techniques are evaluated through simulations in Section IX. Finally, the conclusions are drawn in Section X.

Notations : Matrices, vectors and scalar quantities are denoted by boldface uppercase, boldface lowercase and normal letters, respectively. $a[i]$ and $A[i,j]$ denote the elements i and (i,j) of the vector $\mathbf{a}$ and the matrix $\mathbf{A}$, respectively. Superscripts $(\cdot)^{\mathrm{H}}$, $(\cdot)^{\mathrm{T}}$, $(\cdot)^*$ and $(\cdot)^{-1}$ denote Hermitian, transpose, conjugate operation and the inverse of a matrix, respectively. $\mathbf{I}_N$ is an $N \times N$ identity matrix. $\mathbb{E}\{\cdot\}$ denotes the expectation operator. Symbols $\otimes$ and $\odot$ stand for circular convolution operation and element-wise multiplication, respectively. $\angle a$ indicates the angle of the complex number a, $|a|$ denotes its absolute value, and $||\mathbf{A}||$ is the Frobenius norm of the matrix $\mathbf{A}$. $a := b$ replaces a with b. Finally, $\mathbf{d} = \mathrm{diag}(\mathbf{D})$ is the vector including the elements on the main diagonal of the matrix $\mathbf{D}$,

and $\mathbf{C} = \mathrm{circ}(\mathbf{c})$ is a circulant matrix with the first column $\mathbf{c}$.

II. System Model

Consider the uplink of an OFDM-based massive MIMO system where P single antenna users are communicating with a BS equipped with $M \gg P$ antennas. We assume that different users' wireless channels are statistically independent and time invariant during one OFDM packet. Hence, they can simultaneously share all the available subcarriers as their signals can be distinguished through their respective channel gains. Having N active subcarriers, the $N \times 1$ vector of the κ^{th} OFDM symbol for user p can be obtained as

$$\mathbf{x}_p^{\kappa} = \mathbf{F}_N^{\mathrm{H}} \mathbf{d}_p^{\kappa}, \tag{1}$$

where the $N \times 1$ vector $\mathbf{d}_p^{\kappa}$ contains the κ^{th} data symbol of user p, which is normalized to have a power of unity. Also, $\mathbf{F}_N$ is the normalized N-point DFT matrix with the elements $F_N[i,k] = \frac{1}{\sqrt{N}} e^{-j\frac{2\pi}{N}ik}$ for $i,k = 0, \cdots, N-1$. The CP length, N_{CP}, is considered to be longer than the channel impulse response (CIR) length, L. Also, we consider perfect time synchronization. In addition, we assume a BS with co-located antennas where the BS is equipped with coherent oscillators at all the antennas. Thus, the amount of each user's CFO is the same for all the BS antennas. After CP removal, the OFDM symbol received at the m^{th} BS antenna can be written as

$$\mathbf{r}_m^{\kappa} = \sum_{p=0}^{P-1} \mathbf{\Phi}_p^{\kappa} \mathbf{X}_p^{\kappa} \mathbf{h}_{m,p} + \mathbf{n}_m, \tag{2}$$

where $\mathbf{X}_p^{\kappa}$ is an $N \times L$ matrix including the first L columns of the circulant matrix $\mathrm{circ}(\mathbf{x}_p^{\kappa})$, $\mathbf{n}_m \sim \mathcal{CN}(0, \sigma_n^2 \mathbf{I}_N)$ is the complex additive white Gaussian noise (AWGN) with the variance of σ_n^2 at the m^{th} BS antenna and $\mathbf{h}_{m,p}$ is the $L \times 1$ CIR vector between user p and BS antenna m. We assume the channel taps to be a set of independent and identically distributed (i.i.d.) random variables that follow the complex normal distribution $\mathcal{CN}(0, \boldsymbol{\rho}_p)$, where $\boldsymbol{\rho}_p$ is an $L \times 1$ vector representing the p^{th} user's channel power delay profile (PDP). Also, $\mathbf{\Phi}_p^{\kappa}$ is an $N \times N$ diagonal CFO matrix with the diagonal elements $\Phi_p^{\kappa}[l,l] = e^{j\frac{2\pi}{N}\epsilon_p(l+(N+N_{\mathrm{CP}})\kappa+N_{\mathrm{CP}})}$ for $l = 0, \cdots, N-1$, and ϵ_p is the CFO normalized to subcarrier spacing.

III. CFO Estimation

In this section, we propose a pilot-based CFO estimation technique for OFDM-based massive MIMO systems. We consider the first OFDM symbol within each data packet as users' pilots. To keep the formulation simple, without any loss of generality, we omit the symbol index in our derivations. If we multiply the first received OFDM symbol at each antenna to its Hermitian and average over all the BS antennas, we have the covariance matrix as

$$\begin{aligned}\mathbf{R} &= \frac{1}{M}\sum_{m=0}^{M-1} \mathbf{r}_m \mathbf{r}_m^{\mathrm{H}} \\ &= \sum_{p=0}^{P-1}\sum_{q=0}^{P-1} \mathbf{\Lambda}_p \mathbf{C}_{p,q} \mathbf{\Lambda}_q^{\mathrm{H}} + \frac{1}{M}\sum_{m=0}^{M-1} \mathbf{n}_m \mathbf{n}_m^{\mathrm{H}} \\ &+ \frac{1}{M}\sum_{m=0}^{M-1} (\sum_{p=0}^{P-1} \mathbf{\Lambda}_p \mathbf{h}_{m,p}) \mathbf{n}_m^{\mathrm{H}} + \frac{1}{M}\sum_{m=0}^{M-1} \mathbf{n}_m (\sum_{q=0}^{P-1} \mathbf{\Lambda}_q \mathbf{h}_{m,q})^{\mathrm{H}},\end{aligned} \tag{3}$$

where $\mathbf{\Lambda}_p = \mathbf{\Phi}_p \mathbf{X}_p$ and $\mathbf{C}_{p,q} \triangleq \frac{1}{M}\sum_{m=0}^{M-1} \mathbf{h}_{m,p} \mathbf{h}_{m,q}^{\mathrm{H}}$. In the asymptotic regime, where $M \to \infty$, the last two terms in (3) tend to zero and the second one becomes a diagonal matrix equal to $\sigma_n^2 \mathbf{I}_N$. Hence, for large values of M, $\mathbf{R}$ can be approximated as

$$\mathbf{R} = \sum_{p=0}^{P-1}\sum_{q=0}^{P-1} \mathbf{\Lambda}_p \mathbf{C}_{p,q} \mathbf{\Lambda}_q^{\mathrm{H}} + \sigma_n^2 \mathbf{I}_N. \tag{4}$$

Moreover, according to the law of large numbers, as M grows large, $C_{p,q}[i,j] \to \mathbb{E}\left\{h_{m,p}[i] h_{m,q}^{*}[j]\right\}$.

We denote $\mathbf{P}_{X_q} = \mathbf{I}_N - \mathbf{X}_q (\mathbf{X}_q^{\mathrm{H}} \mathbf{X}_q)^{-1} \mathbf{X}_q^{\mathrm{H}}$ as the orthogonal projection onto the space spanned by the columns of $\mathbf{X}_q$. Then, if we consider the training sequence designed such that $\mathbf{\Lambda}_q^{\perp} = \mathbf{P}_{X_q} \mathbf{\Phi}_q^{\mathrm{H}}$, then, $\mathbf{\Lambda}_q^{\perp} \mathbf{\Lambda}_p = 0$ holds for $q = p$. Therefore, if we estimate CFO, $\hat{\epsilon}_q$, calculate $\hat{\mathbf{\Lambda}}_q^{\perp}$, and multiply it to $\mathbf{R}$, we have

$$\hat{\mathbf{\Lambda}}_q^{\perp} \mathbf{R} = \hat{\mathbf{\Lambda}}_q^{\perp} \mathbf{\Lambda}_q \mathbf{C}_{q,q} \mathbf{\Lambda}_q^{\mathrm{H}} + \hat{\mathbf{\Lambda}}_q^{\perp} \mathbf{V}_q, \tag{5}$$

where

$$\mathbf{V}_q = \sum_{\substack{p=0 \\ p \neq q}}^{P-1} \mathbf{\Lambda}_p \mathbf{C}_{p,p} \mathbf{\Lambda}_p^{\mathrm{H}} + \sigma_n^2 \mathbf{I}_N, \tag{6}$$

denotes the noise plus multi-user interference with respect to user q. Then, if $\hat{\epsilon}_q = \epsilon_q$, the first term in the right-hand side of equation (5) is zero, and the Frobenius norm of the resulting matrix gets its minimum value. Therefore,

$$\hat{\epsilon}_q = \underset{\epsilon}{\mathrm{argmin}} \quad \left\| \hat{\mathbf{\Lambda}}_q^{\perp} \mathbf{R} \right\|^2. \tag{7}$$

The cost function of this optimization problem is a unimodal function, i.e. it is monotonically decreasing for $\epsilon \leq \epsilon_q$ and monotonically increasing for $\epsilon \geq \epsilon_q$. The proof is provided in the Appendix Section. Therefore, this optimization problem can be solved by applying the Golden section search algorithm [31]. This approach is generic, and therefore, there is no restriction on choosing the pilot sequence.

IV. Channel Estimation

Since the focus of this paper is on CFO estimation, we employ a simple ML channel estimation at each BS antenna. To this end, we rearrange equation (2) as

$$\mathbf{r}_m = \mathbf{\Lambda} \mathbf{h}_m + \mathbf{n}_m, \tag{8}$$

where $\mathbf{\Lambda} = [\mathbf{\Lambda}_0, \mathbf{\Lambda}_1, \cdots, \mathbf{\Lambda}_{P-1}]$, and $\mathbf{h}_m = [\mathbf{h}_{m,0}^{\mathrm{T}}, \mathbf{h}_{m,1}^{\mathrm{T}}, \cdots, \mathbf{h}_{m,P-1}^{\mathrm{T}}]^{\mathrm{T}}$. Then, the logarithm of the conditional probability density function (PDF) of $\mathbf{r}_m$ given $\mathbf{h}_m$ and ϵ_q can be written as

$$\ln p(\mathbf{r}_m | \mathbf{h}_{m,p}, \epsilon_q) = \Theta_0 - \Theta_1 [\mathbf{r}_m - \mathbf{\Lambda}\mathbf{h}_{m,p}]^{\mathrm{H}} \times [\mathbf{r}_m - \mathbf{\Lambda}\mathbf{h}_{m,p}], \quad (9)$$

where $\Theta_0 = -N\ln(2\pi\sigma_n^2)/2$, and $\Theta_1 = 1/2\sigma_n^2$. By taking the derivative of equation (9) with respect to $\mathbf{h}_{m,p}$ and setting it equal to zero, the estimated channel can be obtained as

$$\hat{\mathbf{h}}_m = (\mathbf{\Lambda}^{\mathrm{H}}\mathbf{\Lambda})^{-1}\mathbf{\Lambda}^{\mathrm{H}}\mathbf{r}_m. \quad (10)$$

V. CFO COMPENSATION

Unlike other CFO compensation techniques in the literature, we suggest to compensate the users' CFOs after combining the received signals at BS antennas. In fact, if the CFO compensation is performed before channel equalization, the CFOs should be compensated separately for all the received signals at M BS antennas. As the number of BS antennas grows large, CFO compensation can impose a considerable amount of complexity to the system, as we need a separate OFDM receiver per antenna per user. In this section, we propose a CFO compensation technique that can be performed only once for each user, and consequently, its computational complexity is independent of the number of BS antennas.

Representing the circular convolution of the transmit data with the channel as $\mathbf{H}_{m,p}\mathbf{x}_p$, the received signal at BS antenna m in the frequency domain can be written as

$$\bar{\mathbf{r}}_m = \sum_{p=0}^{P-1} \mathbf{F}_N \mathbf{\Phi}_p \mathbf{H}_{m,p}\mathbf{x}_p + \mathbf{F}_N\mathbf{n}_m, \quad (11)$$

where $\mathbf{H}_{m,p}$ is a circulant matrix with the first column $\mathbf{h}_{m,p}$ which is zero-padded to have the length of N. Considering $\mathbf{F}_N^{\mathrm{H}}\mathbf{F}_N = \mathbf{I}_N$, equation (11) can be rewritten as

$$\bar{\mathbf{r}}_m = \sum_{p=0}^{P-1} \mathbf{F}_N \mathbf{\Phi}_p \mathbf{F}_N^{\mathrm{H}}\mathbf{F}_N\mathbf{H}_{m,p}\mathbf{F}_N^{\mathrm{H}}\mathbf{d}_p + \bar{\mathbf{n}}_m, \quad (12)$$

where $\bar{\mathbf{n}}_m = \mathbf{F}_N\mathbf{n}_m$ is the frequency domain noise vector. By defining $\mathbf{E}_p \triangleq \mathbf{F}_N\mathbf{\Phi}_p\mathbf{F}_N^{\mathrm{H}}$ and $\widetilde{\mathbf{H}}_{m,p} \triangleq \mathbf{F}_N\mathbf{H}_{m,p}\mathbf{F}_N^{\mathrm{H}}$, we have

$$\bar{\mathbf{r}}_m = \sum_{p=0}^{P-1} \mathbf{E}_p\widetilde{\mathbf{H}}_{m,p}\mathbf{d}_p + \bar{\mathbf{n}}_m. \quad (13)$$

It is worth noting that due to the circulant property of $\mathbf{H}_{m,p}$, $\widetilde{\mathbf{H}}_{m,p}$ becomes a diagonal matrix, [32].

Let us define the vector $\bar{\mathbf{r}}[k] = [\bar{r}_0[k], \bar{r}_1[k], \cdots, \bar{r}_{M-1}[k]]^{\mathrm{T}}$ which contains the k^{th} samples of the received signals at all the BS antennas in the frequency domain for $k = 0, 1, \cdots, N-1$. Then, the combiner output is given by

$$\bar{\mathbf{y}}[k] = \mathbf{Z}[k]\bar{\mathbf{r}}[k], \quad (14)$$

where $\bar{\mathbf{y}}[k] = [\bar{y}_0[k], \bar{y}_1[k], \cdots, \bar{y}_{P-1}[k]]^{\mathrm{T}}$ is a $P \times 1$ vector containing the k^{th} samples of the users' signals, and $\mathbf{Z}[k]$ is a $P \times M$ linear combiner on subcarrier k. If we deploy the zero-forcing (ZF) combiner, $\mathbf{Z}[k]$ can be calculated as

$$\mathbf{Z}[k] = (\boldsymbol{\mathcal{H}}[k]^{\mathrm{H}}\boldsymbol{\mathcal{H}}[k])^{-1}\boldsymbol{\mathcal{H}}^{\mathrm{H}}[k], \quad (15)$$

where $\boldsymbol{\mathcal{H}}[k] = [\bar{\mathbf{h}}_0[k], \bar{\mathbf{h}}_1[k], \cdots, \bar{\mathbf{h}}_{P-1}[k]]$ is an $M \times P$ matrix whose p^{th} column is $\bar{\mathbf{h}}_p[k] = [\bar{h}_{0,p}[k], \bar{h}_{1,p}[k], \cdots, \bar{h}_{M-1,p}[k]]^{\mathrm{T}}$, and $\bar{\mathbf{h}}_{m,p} = \mathbf{F}_N\mathbf{h}_{m,p}$.

Note that in the asymptotic regime, $P \times P$ normalization matrix $\boldsymbol{\mathcal{H}}[k]^{\mathrm{H}}\boldsymbol{\mathcal{H}}[k]$ becomes a diagonal matrix,

$$\mathbf{D}_k = \boldsymbol{\mathcal{H}}[k]^{\mathrm{H}}\boldsymbol{\mathcal{H}}[k] = \mathrm{diag}\left\{\left\|\bar{\mathbf{h}}_0[k]\right\|^2, \left\|\bar{\mathbf{h}}_1[k]\right\|^2, \cdots, \left\|\bar{\mathbf{h}}_{P-1}[k]\right\|^2\right\}, \quad (16)$$

and when M tends to infinity, according to the law of large numbers, $\mathbf{D}_k \to N\mathbf{I}_P$. Therefore, the combiner output for user q can be written as

$$\bar{y}_q[k] = \frac{1}{N}\bar{\mathbf{h}}_q^{\mathrm{H}}[k]\bar{\mathbf{r}}[k], \quad (17)$$

for $k = 0, 1, \cdots, N-1$. Substituting $\bar{\mathbf{r}}$ from (13) into (17), we can rewrite the q^{th} user's signal at the combiner output as

$$\bar{\mathbf{y}}_q = \frac{1}{N}\sum_{m=0}^{M-1}\widetilde{\mathbf{H}}_{m,q}^{\mathrm{H}}\sum_{p=0}^{P-1}\mathbf{E}_p\widetilde{\mathbf{H}}_{m,p}\mathbf{d}_p + \tilde{\mathbf{n}}, \quad (18)$$

where $\tilde{\mathbf{n}} = \frac{1}{N}\sum_{m=0}^{M-1}\widetilde{\mathbf{H}}_{m,q}^{\mathrm{H}}\bar{\mathbf{n}}_m$. Then, defining an $N \times N$ interference matrix as

$$\mathbf{\Omega}_{q,p} = \frac{1}{N}\sum_{m=0}^{M-1}\widetilde{\mathbf{H}}_{m,q}^{\mathrm{H}}\mathbf{E}_p\widetilde{\mathbf{H}}_{m,p}, \quad (19)$$

we have

$$\bar{\mathbf{y}}_q = \mathbf{\Omega}_{q,q}\mathbf{d}_q + \sum_{\substack{p=0 \\ p\neq q}}^{P-1}\mathbf{\Omega}_{q,p}\mathbf{d}_p + \tilde{\mathbf{n}}, \quad (20)$$

It is worth noting that since different users' channels are uncorrelated, the elements of $\mathbf{\Omega}_{q,p}$ for $p \neq q$ tend to zero as M increases to infinity, and multi-user interference as well as the noise term will be averaged out. Moreover, while in the absence of CFO, $\mathbf{\Omega}_{q,q}$ is the identity matrix, the presence of CFO makes it non-diagonal and banded, with the off-diagonal elements modeling the inter-carrier interference (ICI) effect. Furthermore, with some manipulations, the interference matrix in equation (19) can be represented as

$$\mathbf{\Omega}_{q,p} = \mathbf{E}_p \odot \mathbf{B}_{q,p}, \quad (21)$$

where

$$B_{q,p}[l,k] = \frac{1}{N}\sum_{m=0}^{M-1}\widetilde{H}_{m,q}^{*}[l,l]\widetilde{H}_{m,p}[k,k], \quad (22)$$

for $l, k = 0, \cdots, N-1$. Therefore, in the asymptotic regime $\mathbf{B}_{q,q}$ can be obtained as

$$\begin{aligned} B_{q,q}[l,k] &= \mathbb{E}\left\{\widetilde{H}_{m,q}^{*}[l,l]\widetilde{H}_{m,q}[k,k]\right\} \\ &= \mathbb{E}\left\{\bar{h}_{m,q}^{*}[l]\bar{h}_{m,q}[k]\right\} \\ &= \mathbb{E}\left\{\sum_{i=0}^{N-1}\sum_{i'=0}^{N-1}h_{m,q}^{*}[i]h_{m,q}[i']\,e^{-j\frac{2\pi}{N}(ki'-li)}\right\}. \end{aligned} \quad (23)$$

and $\mathbb{E}\left\{h^*_{m,q}[i]h_{m,q}[i']\right\}=0$ for $i\neq i'$ since $\mathbf{h}_{m,q}$ is an i.i.d. random vector, and we have

$$B_{q,q}[l,k]=\sum_{i=0}^{N-1}\rho_q[i]e^{-j\frac{2\pi}{N}(k-l)i}=\bar{\rho}_q[k-l], \tag{24}$$

where $\bar{\boldsymbol{\rho}}_q=\mathbf{F}_N\boldsymbol{\rho}_q$ contains the N-point DFT samples of the channel PDP of the q^{th} user, $\boldsymbol{\rho}_q$, and since the channel PDPs are real-valued functions, $\bar{\rho}_q[i]=\bar{\rho}_q[i-N]$. Hence, we can conclude that $\mathbf{B}_{q,q}$ is a circulant matrix with the first column $\bar{\rho}_q[-l]$ for $l=0,\cdots,N-1$. $\mathbf{E}_q=\mathbf{F}_N\boldsymbol{\Phi}_q\mathbf{F}_N^{\text{H}}$ is also a circulant matrix as $\boldsymbol{\Phi}_q$ is diagonal. Accordingly, $\boldsymbol{\Omega}_{q,q}$ derived in equation (21), is a circulant matrix and can be written as $\boldsymbol{\Omega}_{q,q}=\mathbf{F}_N\mathbf{Q}_{q,q}\mathbf{F}_N^{\text{H}}$, where $\mathbf{Q}_{q,q}$ is diagonal. Therefore, in order to calculate the inverse of the interference matrix, $\boldsymbol{\Omega}_{q,q}$, we only need to calculate the inverse of the diagonal matrix $\mathbf{Q}_{q,q}$, and calculate, $\boldsymbol{\Omega}_{q,q}^{-1}=\mathbf{F}_N\mathbf{Q}_{q,q}^{-1}\mathbf{F}_N^{\text{H}}$. Moreover, due to the circulant property of the matrix $\boldsymbol{\Omega}_{q,q}$, calculating its first column, which is the element-wise multiplication of the first columns of the matrices $\mathbf{E}_p$ and $\mathbf{B}_{q,p}$, is sufficient to form the rest of this matrix. Since an element-wise multiplication in the frequency domain is equivalent to a circular convolution in the time domain, the diagonal elements of the matrix $\mathbf{Q}_{q,q}$ can be obtained as

$$\text{diag}(\mathbf{Q}_{q,q})=\text{diag}(\boldsymbol{\Phi}_q)\otimes\tilde{\boldsymbol{\rho}}_q, \tag{25}$$

where $\tilde{\boldsymbol{\rho}}_q[i]=\boldsymbol{\rho}_q[-i]=\boldsymbol{\rho}_q[N-i]$. Hence, the q^{th} user's signal can be obtained as

$$\hat{\mathbf{d}}_q=\mathbf{F}_N\mathbf{Q}_{q,q}^{-1}\mathbf{F}_N^{\text{H}}\bar{\mathbf{y}}_q. \tag{26}$$

Considering the symbol indices, one realizes that $\mathbf{Q}_{q,q}$ varies for different symbols as

$$\text{diag}(\mathbf{Q}_{q,q}^{\kappa})=\text{diag}(\boldsymbol{\Phi}_q^{\kappa})\otimes\tilde{\boldsymbol{\rho}}_q. \tag{27}$$

To deal with this issue, we suggest to calculate the matrix $\mathbf{Q}_{q,q}$ once for the first symbol, where $\Phi_q^0[l,l]=e^{j\frac{2\pi}{N}\epsilon_p(l+N_{\text{CP}})}$ for $l=0,1,\cdots,N-1$, and for other symbols add a phase shift correction step. Thus, the κ^{th} data symbol can be estimated as

$$\hat{\mathbf{d}}_q^{\kappa}=e^{-j\frac{2\pi}{N}\epsilon_q(N+N_{\text{CP}})\kappa}\mathbf{F}_N\mathbf{Q}_{q,q}^{-1}\mathbf{F}_N^{\text{H}}\bar{\mathbf{y}}_q^{\kappa}, \tag{28}$$

It is worth to note that our proposed CFO compensation technique is performed only once for each user, and as a result, its computational complexity remains constant as the number of BS antennas increases.

VI. CFO Estimation Error Analysis

In Section V, we have assumed that the CFO estimation is accurate. In this section, we analyze the effect of CFO estimation errors and investigate the efficacy of the proposed technique. We consider the estimated CFO for user p as $\hat{\epsilon}_p=\epsilon_p+\tilde{\epsilon}_p$ where $\tilde{\epsilon}_p$ is the estimation error. Thus, the estimated CFO matrix can be written as

$$\hat{\boldsymbol{\Phi}}_p=\tilde{\boldsymbol{\Phi}}_p\boldsymbol{\Phi}_p, \tag{29}$$

where $\tilde{\boldsymbol{\Phi}}_p$ is a diagonal matrix with the elements $\tilde{\Phi}_p^{\kappa}[l,l]=e^{j\frac{2\pi}{N}\tilde{\epsilon}_p(l+(N+N_{\text{CP}})\kappa+N_{\text{CP}})}$ for $l=0,\cdots,N-1$. After dropping the superscript κ for the sake of simplicity without loss of generality, the estimated channel at the m^{th} BS antenna can be obtained from equation (10) as

$$\begin{aligned}\hat{\mathbf{h}}_m=&(\hat{\boldsymbol{\Lambda}}^{\text{H}}\hat{\boldsymbol{\Lambda}})^{-1}\hat{\boldsymbol{\Lambda}}^{\text{H}}\mathbf{r}_m\\=&(\hat{\boldsymbol{\Lambda}}^{\text{H}}\hat{\boldsymbol{\Lambda}})^{-1}\hat{\boldsymbol{\Lambda}}^{\text{H}}\boldsymbol{\Lambda}\mathbf{h}_m+(\hat{\boldsymbol{\Lambda}}^{\text{H}}\hat{\boldsymbol{\Lambda}})^{-1}\hat{\boldsymbol{\Lambda}}^{\text{H}}\mathbf{n}_m,\end{aligned} \tag{30}$$

where $\hat{\boldsymbol{\Lambda}}=[\hat{\boldsymbol{\Lambda}}_0,\hat{\boldsymbol{\Lambda}}_1,\cdots,\hat{\boldsymbol{\Lambda}}_{P-1}]$ and $\hat{\boldsymbol{\Lambda}}_p=\hat{\boldsymbol{\Phi}}_p\mathbf{X}_p$. Let us define $NP\times NP$ matrices $\boldsymbol{\Gamma}_1\triangleq\hat{\boldsymbol{\Lambda}}^{\text{H}}\hat{\boldsymbol{\Lambda}}$ and $\boldsymbol{\Gamma}_2\triangleq\hat{\boldsymbol{\Lambda}}^{\text{H}}\boldsymbol{\Lambda}$, with the elements

$$\begin{aligned}\Gamma_1[i,j]=&\sum_{l=0}^{N-1}\hat{\Lambda}_p^*[i,l]\hat{\Lambda}_q[l,j]\\=&\sum_{l=0}^{N-1}X_p^*[l,i-pN]\Phi_p^*[l,l]\tilde{\Phi}_p^*[l,l]\tilde{\Phi}_q[l,l]\Phi_q[l,l]\\&\times X_q[l,j-qN],\end{aligned} \tag{31}$$

and

$$\begin{aligned}\Gamma_2[i,j]=&\sum_{l=0}^{N-1}\hat{\Lambda}_p^*[i,l]\Lambda_q[l,j]\\=&\sum_{l=0}^{N-1}X_p^*[l,i-pN]\Phi_p^*[l,l]\tilde{\Phi}_p^*[l,l]\Phi_q[l,l]X_q[l,j-qN].\end{aligned} \tag{32}$$

Here, p and q can be obtained as $p=\lfloor\frac{i}{N}\rfloor$ and $q=\lfloor\frac{j}{N}\rfloor$. Therefore, if $|i-j|<N$, $q=p$ and we have

$$\Gamma_1[i,j]=\begin{cases}1, & i=j\\ 0, & i\neq j,\end{cases} \tag{33}$$

and

$$\Gamma_2[i,j]=\sum_{l=0}^{N-1}\tilde{\Phi}_p^*[l,l]X_p^*[l,i-pN]X_p[l,j-pN]. \tag{34}$$

It is worth noting that when the estimation error, $\tilde{\epsilon}_p$, has a small value, for $i\neq j$, $\Gamma_2[i,j]\approx 0$, and for $i=j$, we have

$$\Gamma_2[i,i]=\sum_{l=0}^{N-1}\tilde{\Phi}_p^*[l,l]\Big|X_p[l,i-pN]\Big|^2. \tag{35}$$

Then, according to the Parseval's theorem, we can rewrite equation (35) as

$$\Gamma_2[i,i]=\frac{1}{N}\sum_{k=0}^{N-1}\widetilde{E}_p^*[k,0]\Big|d_p[k]\Big|^2, \tag{36}$$

where $|d_p[k]|=1$, and $\widetilde{\mathbf{E}}_p=\mathbf{F}_N\tilde{\boldsymbol{\Phi}}_p\mathbf{F}_N^{\text{H}}$ is a circulant matrix, and its first column is the Fourier transform of $\text{diag}(\tilde{\boldsymbol{\Phi}}_{\text{p}})$. Moreover, with the assumption of small $\tilde{\epsilon}_p$, the first column of $\widetilde{\mathbf{E}}_p$ can be considered as an impulse, i.e., $\widetilde{E}_p^*[k,0]\approx\widetilde{E}_p^*[0,0]\delta[k]$. Hence, for $|i-j|<N$,

$$\Gamma_2[i,j]\approx\begin{cases}\varphi_p^*, & i=j\\ 0, & i\neq j,\end{cases} \tag{37}$$

where

$$\varphi_p=\frac{1}{N}\widetilde{E}_p[0,0]=\frac{1}{N}\sum_{l=0}^{N-1}\tilde{\Phi}_p[l,l]. \tag{38}$$

Since the estimation is performed on the first symbol, i.e. $\kappa = 0$, which is the pilot, we can expand equation (38) as

$$\begin{aligned}\varphi_p &= \frac{1}{N}\sum_{l=0}^{N-1} e^{j\frac{2\pi}{N}\tilde{\epsilon}_p(l+N_{\mathrm{CP}})} \\ &= \frac{1}{N}\sum_{l=0}^{N-1}\left\{\cos\left(\frac{2\pi}{N}\tilde{\epsilon}_p l\right)+j\sin\left(\frac{2\pi}{N}\tilde{\epsilon}_p l\right)\right\} e^{j\frac{2\pi}{N}\tilde{\epsilon}_p N_{\mathrm{CP}}}.\end{aligned} \tag{39}$$

Due to the small value of $\tilde{\epsilon}_p$, we can replace $\cos\left(\frac{2\pi}{N}\tilde{\epsilon}_p l\right) = 1$ and $\sin\left(\frac{2\pi}{N}\tilde{\epsilon}_p l\right) = \frac{2\pi}{N}\tilde{\epsilon}_p l$. Thus,

$$\begin{aligned}\varphi_p &= \frac{1}{N}\sum_{l=0}^{N-1}\left\{1+j\frac{2\pi}{N}\tilde{\epsilon}_p l\right\} e^{j\frac{2\pi}{N}\tilde{\epsilon}_p N_{\mathrm{CP}}} \\ &= \left(1+j\frac{2\pi}{N}\tilde{\epsilon}_p\frac{N-1}{2}\right)e^{j\frac{2\pi}{N}\tilde{\epsilon}_p N_{\mathrm{CP}}} \\ &= \left\{\cos\left(\frac{2\pi}{N}\tilde{\epsilon}_p\frac{N-1}{2}\right)+j\sin\left(\frac{2\pi}{N}\tilde{\epsilon}_p\frac{N-1}{2}\right)\right\} e^{j\frac{2\pi}{N}\tilde{\epsilon}_p N_{\mathrm{CP}}} \\ &= e^{j\frac{2\pi}{N}\tilde{\epsilon}_p(\frac{N-1}{2}+N_{\mathrm{CP}})} \\ &= \tilde{\Phi}_p[l,l]\big|_{l=\frac{N-1}{2}}.\end{aligned} \tag{40}$$

Therefore, with a similar argument, if we replace $\tilde{\Phi}_p[l,l]$ for $l = 0, 1, \cdots, N-1$ with $\tilde{\Phi}_p[\frac{N}{2}, \frac{N}{2}]$ in equation (32), we can also consider $\Gamma_2[i,j] \approx \varphi_p^* \Gamma_1[i,j]$ for $|i-j| \geq N$. Note that since N is set as an even number, and consequently, $\frac{N-1}{2}$ is not an integer, we have chosen $\frac{N}{2} = \lceil\frac{N-1}{2}\rceil$. Then, we can conclude $\mathbf{\Gamma}_1^{-1}\mathbf{\Gamma}_2 \approx [\varphi_0^* I_N, \varphi_1^* I_N, \cdots, \varphi_P^* I_N]$. Hence, the estimated channels that are used for the ZF combiner can be written as

$$\hat{\mathbf{h}}_{m,p} = \varphi_p^* \mathbf{h}_{m,p} + \breve{\mathbf{n}}_m, \tag{41}$$

where $\breve{\mathbf{n}}_m = (\hat{\mathbf{\Lambda}}^{\mathrm{H}}\hat{\mathbf{\Lambda}})^{-1}\hat{\mathbf{\Lambda}}^{\mathrm{H}}\mathbf{n}_m$. By ignoring the MUI and the noise term in equation (20) due to their small values, the combined signal of user q is given by

$$\bar{\mathbf{y}}_q = \widetilde{\mathbf{\Omega}}_{q,q}\mathbf{d}_p, \tag{42}$$

where $\widetilde{\mathbf{\Omega}}_{q,q} = \mathbf{E}_q \odot \widetilde{\mathbf{B}}_{q,q}$ and the elements of $\widetilde{\mathbf{B}}_{q,q}$ can be obtained as

$$\begin{aligned}\widetilde{B}_{q,q}[l,k] =& \mathbb{E}\left\{\sum_{i=0}^{N-1}\hat{h}^*_{m,q}[i]h_{m,q}[i]e^{-j\frac{2\pi}{N}(k-l)i}\right\} \\ =& \varphi_q\sum_{i=0}^{N-1}\mathbb{E}\left\{h^*_{m,q}[i]h_{m,q}[i]\right\}e^{-j\frac{2\pi}{N}(k-l)i} \\ =& \varphi_q\bar{\rho}_q[k-l],\end{aligned} \tag{43}$$

With a similar argument as in Section V, one can prove that $\widetilde{\mathbf{\Omega}}_{q,q}$ is a circulant matrix and can be written as $\widetilde{\mathbf{\Omega}}_{q,q} = \mathbf{F}_N\widetilde{\mathbf{Q}}_{q,q}\mathbf{F}_N^{\mathrm{H}}$, where $\widetilde{\mathbf{Q}}_{q,q}$ is a diagonal matrix with the main diagonal elements

$$\begin{aligned}\widetilde{Q}_{q,q}[i,i] &= \sum_{n=0}^{N-1}\varphi_q\tilde{\rho}_q[i-n]\Phi_q[n,n] \\ &= \varphi_q Q_{q,q}[i,i].\end{aligned} \tag{44}$$

Consequently, in the proposed CFO compensation, we need to calculate the interference matrix using the estimated values of the CFOs and channel impulse responses, i.e. $\widehat{\mathbf{\Omega}}_{q,p} = \widehat{\mathbf{E}}_q \odot \widehat{\mathbf{B}}_{q,p}$. Similarly, the elements of the matrix $\widehat{\mathbf{B}}_{q,p}$ are calculated as

$$\begin{aligned}\widehat{B}_{q,q}[l,k] =& \mathbb{E}\left\{\sum_{i=0}^{N-1}\hat{h}^*_{m,q}[i]\hat{h}_{m,q}[i]e^{-j\frac{2\pi}{N}(k-l)i}\right\} \\ =& \bar{\rho}_q[k-l],\end{aligned} \tag{45}$$

which is equal to $B_{q,q}[l,k]$ in the case of accurate CFO estimation. Using the result in (40), it can be shown that

$$\widehat{\mathbf{E}}_q = \mathbf{F}_N\hat{\mathbf{\Phi}}_p\mathbf{F}_N^{\mathrm{H}} = \varphi_q\mathbf{E}_q, \tag{46}$$

and consequently, $\widehat{\mathbf{Q}}_{q,q} = \widetilde{\mathbf{Q}}_{q,q} = \varphi_q\mathbf{Q}_{q,q}$. As a result, the calculated interference matrix from the estimated values, $\widehat{\mathbf{\Omega}}_{q,q}$, is equal to the interference matrix in the case of inaccurate CFO estimation, $\widetilde{\mathbf{\Omega}}_{q,q}$. Thus, by multiplying $\widehat{\mathbf{\Omega}}_{q,q}^{(-1)}$ to equation (42), the q^{th} user's signal, $\mathbf{d}_q$, can be extracted. As it is mentioned in Section V, $\widehat{\mathbf{Q}}_{q,q}$ is calculated only for the first symbol, and the phase shift of other symbols are corrected later. Thus, the data of the κ^{th} symbol can be obtained as

$$\begin{aligned}\hat{\mathbf{d}}_q^\kappa &= e^{-j\frac{2\pi}{N}(\hat{\epsilon}_q-\epsilon_q)(N+N_{\mathrm{CP}})\kappa}\widehat{\mathbf{\Omega}}_{q,q}^{(-1)}\widetilde{\mathbf{\Omega}}_{q,q}\mathbf{d}_q^\kappa \\ &= e^{-j\frac{2\pi}{N}\tilde{\epsilon}_q(N+N_{\mathrm{CP}})\kappa}\mathbf{d}_q^\kappa,\end{aligned} \tag{47}$$

Therefore, by applying the proposed CFO compensation technique, the estimation error is absorbed into the interference matrix, and after compensation only a phase shift remains.

It is worth mentioning that though the residual phase shift in our proposed compensation technique is small, it progressively increases symbol by symbol, and it can result in a large rotation of the constellation. In the next section, a phase correction technique is proposed to calculate and effectively eliminate this error.

VII. CFO Estimation Error correction

In this section, we suggest an approach to efficiently compensate the phase shift due to CFO estimation error. As it was discussed earlier, this error is zero for the first symbol and we cannot use the pilot to calculate this shift. Thus, we need to compare the users' signals with the constellation points and find the closest point as

$$\begin{aligned}\check{d}_q^\kappa[k] =& \underset{c}{\mathrm{argmin}}|\hat{d}_q^\kappa[k]-c|. \\ & \text{s.t.} \quad c\in\mathbb{S}\end{aligned} \tag{48}$$

where $\mathbb{S}$ is the set of all the possible constellation points. Then, from equation (47), the estimation error can be calculated as

$$\tilde{\epsilon}_q = \frac{1}{2\pi(N+N_{\mathrm{CP}})\kappa}\sum_{k=0}^{N-1}\angle\check{d}_q^\kappa[k]-\angle\hat{d}_q^\kappa[k]. \tag{49}$$

where $\kappa \neq 0$. After calculating the error, we can correct the phase shift error for the current symbol as

$$\hat{\mathbf{d}}_p^\kappa := e^{j\frac{2\pi}{N}\tilde{\epsilon}_q(N+N_{\mathrm{CP}})\kappa}\hat{\mathbf{d}}_q^\kappa, \tag{50}$$

and update the estimated CFO for the phase correction step of the following symbols as $\hat{\epsilon}_q := \hat{\epsilon}_q - \tilde{\epsilon}_q$. In the asymptotic regime, the error can be calculated precisely. Thus, after

updating the estimated CFO, $\hat{\epsilon}_q$, for one symbol, there will be no phase shift error on the following symbols. However, in practice when M is not very large, MUI and noise are not completely averaged out, and the CFO estimation error in general cannot be accurately calculated and corrected. To deal with this issue, we can execute the correction loop for more than one symbol. The CFO compensation process with error correction for $N_{\rm cor}$ number of symbols from $N_{\rm sym}$ transmitted symbols is presented in Algorithm 1.

Algorithm 1 CFO compensation with error correction

Calculate $\mathbf{Q}_{q,q}^{0}$ from equation (27)
for $\kappa = 0, 1, \cdots, N_{\rm sym}$ **do**
  $\hat{\mathbf{d}}_q^{\kappa} = e^{-j\frac{2\pi}{N}\hat{\epsilon}_p(N+N_{\rm CP})\kappa}\mathbf{F}_N(\mathbf{Q}_{q,q}^{0})^{-1}\mathbf{F}_N^{\rm H}\bar{\mathbf{y}}_q^{\kappa}$
  if $1 \le \kappa \le N_{\rm cor}+1$ **then**
    Calculate $\check{d}_q^{\kappa}$ from equation (48)
    Calculate $\tilde{\epsilon}_q$ from equation (49)
    $\hat{\mathbf{d}}_p^{\kappa} := e^{j\frac{2\pi}{N}\tilde{\epsilon}_q(N+N_{\rm CP})\kappa}\hat{\mathbf{d}}_q^{\kappa}$
    $\hat{\epsilon}_q := \hat{\epsilon}_q - \tilde{\epsilon}_q$
  end
end

It should be noted that since $\tilde{\epsilon}_q$ is small, most of the elements in the received symbol fall in the correct decision areas. However, for large constellation sizes, even a small phase shift might cause some errors. We suggest to repeat the process of error calculation and correction until we get the error equal to zero. In fact, in each iteration, since we turn the constellation, a larger number of points will fall in their respective decision areas, and an improved phase shift error calculation can be achieved. Algorithm 2 summarizes the CFO compensation process with iterative error correction, where ξ indicates the convergence tolerance.

Algorithm 2 CFO compensation with iterative error correction

Calculate $\mathbf{Q}_{q,q}^{0}$ from equation (27)
for $\kappa = 0, 1, \cdots, N_{\rm sym}$ **do**
  $\hat{\mathbf{d}}_q^{\kappa} = e^{-j\frac{2\pi}{N}\hat{\epsilon}_p(N+N_{\rm CP})\kappa}\mathbf{F}_N(\mathbf{Q}_{q,q}^{0})^{-1}\mathbf{F}_N^{\rm H}\bar{\mathbf{y}}_q^{\kappa}$
  if $1 \le \kappa \le N_{\rm cor}+1$ **then**
    while $\tilde{\epsilon}_q > \xi$ **do**
      Calculate $\check{d}_q^{\kappa}$ from equation (48)
      Calculate $\tilde{\epsilon}_q$ from equation (49)
      $\hat{\mathbf{d}}_p^{\kappa} := e^{j\frac{2\pi}{N}\tilde{\epsilon}_q(N+N_{\rm CP})\kappa}\hat{\mathbf{d}}_q^{\kappa}$
      $\hat{\epsilon}_q := \hat{\epsilon}_q - \tilde{\epsilon}_q$
    end
  end
end

VIII. Computational Complexity

According to our proposed frequency synchronization technique, the CFO estimation is performed in the time domain, and the CFO compensation takes place after combining the received signals over all the BS antennas in the frequency domain. It means that unlike the other existing synchronization techniques, in our case, one set of DFT operations can be used for all the user signals and the separate receivers are not required. Therefore, ignoring the complexity of the channel estimation, the total number of complex multiplications (CMs) done at the receiver with the proposed synchronization technique can be denoted as

$$\mathcal{C}_{\rm p} = \mathcal{C}_{\rm p}^{\rm Est} + M\mathcal{C}^{\rm DFT} + P\mathcal{C}^{\rm Comb} + P\mathcal{C}_{\rm p}^{\rm Comp}, \qquad (51)$$

where $\mathcal{C}_{\rm p}^{\rm Est}$, $\mathcal{C}^{\rm DFT}$, $\mathcal{C}^{\rm Comb}$, and $\mathcal{C}_{\rm p}^{\rm Comp}$ are the number of CMs required for our proposed CFO estimation technique, DFT operation, signal combiner, and our proposed CFO compensation technique, respectively.

For our proposed CFO estimation, the matrix $\mathbf{R}$ in equation (3) is calculated with MN^2 CMs. Then, calculating the cost function for each trial CFO requires N^2 CMs for the matrix in equation (5) and N CMs for the Frobenius norm of the resulting matrix. Therefore, the total computational complexity of our proposed estimation is given by

$$\mathcal{C}_{\rm p}^{\rm Est} = MN^2 + i_c P(N^2+N), \qquad (52)$$

where i_c is the number of trial CFO in the Golden search algorithm. Afterward, the complexity of DFT operation is $\mathcal{C}^{\rm DFT} = \frac{N}{2}\log_2 N$ if FFT is exploited, and the complexity of the utilized ZF combiner is $\mathcal{C}^{\rm Comb} = 3NMP^2$.

For our proposed CFO compensation, first, we need to obtain the matrix $\boldsymbol{Q}_{q,q}$, which requires NL number of CMs due to the circular convolution process introduced in equation (25). Note that $\mathbf{B}_{q,q}$ and $\mathbf{E}_q$ are both circulant matrices with the first column $\bar{\boldsymbol{\rho}}^*$ and the DFT of the main diagonal of $\boldsymbol{\Phi}_q$, i.e., $\mathbf{F}_N{\rm diag}(\boldsymbol{\Phi}_q)$, respectively. Thus, we only need two DFT operations to calculate their first columns, and then we can form the entire matrices. Since the multiplication of two circulant matrices is also a circulant matrix, for the element-wise multiplication in (21), only N number of CMs are required to obtain the first column of $\boldsymbol{\Omega}_{q,q}$, which is the DFT of the main diagonal of $\mathbf{Q}_{q,q}$. Afterward, as it is indicated in equation (28), we take $\bar{\mathbf{y}}_q$ to the time domain, divide it element-wise by the elements on the main diagonal of $\mathbf{Q}_{q,q}$, and bring it back to the frequency domain. Therefore, two N-point IDFT operations, N number of CMs and one N-point DFT operation are needed to obtain the compensated signal. At the end, $i_p N N_{\rm cor}$ number of CMs is required if the phase correction algorithm performs over $N_{\rm cor}$ OFDM symbols, where i_p is the number of iterations. Therefore, the number of required CMs for our proposed compensation technique is

$$\mathcal{C}_p^{\rm Comp} = N(\log_2 N + L + 1 + i_p N_{\rm cor}). \qquad (53)$$

As a comparison, in all the other existing synchronization techniques, the CFO compensation is performed in the time domain by multiplying the compensation vector of the desired user, i.e., ${\rm diag}(\boldsymbol{\Phi}_{\rm q}^{\rm H})$ to the received signals at the BS antennas. Thus, $\mathcal{C}_{\rm t}^{\rm Comp} = MN$ number of CMs are required for CFO compensation, which increase linearly with the number of BS antennas, M; the computational complexity of our CFO compensation technique is instead independent of the number of BS antennas and stays constant if M grows. In addition, each user needs a separate set of DFT operations. Hence, the

total computational complexity of the receiver can be obtained by

$$\mathcal{C} = \mathcal{C}^{\text{Est}} + PMC^{\text{DFT}} + P\mathcal{C}^{\text{Comb}} + P\mathcal{C}_{\text{t}}^{\text{Comp}}, \tag{54}$$

where $\mathcal{C}^{\text{DFT}}$ and $\mathcal{C}^{\text{Comb}}$ are the same as in equation (51).

Regarding the CFO estimation, the number of required CMs of the lowest computationally complex technique in the literature, [29], is given by

$$\mathcal{C}_1^{\text{Est}} = 2M(N - PL) + P. \tag{55}$$

However, the performance of the technique in [29] relies on the long pilot sequences. As it is presented in Section IX, with the same pilot length, our proposed technique can provide a considerably better performance. Later, the work in [30], proposed a rather low-complexity CFO estimation technique in which the number of required CMs is obtained by

$$\mathcal{C}_2^{\text{Est}} = PMN^{(5/2)}. \tag{56}$$

Note that by increasing the number of BS antennas, the computational complexity of the technique in [30] grows with the slope of $PN^{(5/2)}$, while the slope in our case is only N^2 which is also independent of the number of users. More recently a scattered pilot-based frequency synchronization was proposed in [25] that uses N_p out of N subcarriers as pilots. It is also considered that the channels and CFOs of all users stay constant over L_b OFDM blocks. Then, the number of required CMs for the CFO estimation is obtained as

$$\begin{aligned}\mathcal{C}_3^{\text{Est}} &= i_c P(L_b NM \log_2 N + M(L_b - 1)N_p + 6P \\ &\times (L_b NM \log_2 N + (L_b - 1)M^2 N_p/2 + M^3)) \\ &+ L_b NM^2/2 + M^3.\end{aligned} \tag{57}$$

In addition, a computationally efficient blind CFO estimation is proposed in [27] that considers N_0 out of N subcarriers as null subcarriers. Then, its total computational complexity is equal to

$$\begin{aligned}\mathcal{C}_4^{\text{Est}} &= P(i_c(L_b MN \log_2 N + M^3 + M^2 N_0 L_b/2) \\ &+ 3(L_b MN \log_2 N + M^2 N_0 L_b/2 + L_b M_e MN + M^3) \\ &+ 11(L_b M_e N \log_2 N + M_e L_b N + NM_e^2 L_b/2) \\ &+ 3\binom{M_e}{2}8N + 8NM_e^3),\end{aligned} \tag{58}$$

where $M_e = M - (P-1)L$.

As an illustration, a numerical comparison of all the aforementioned CFO estimation techniques is provided in table I. We consider $P = 4$ users, $N = 256$ subcarriers, and CIR length of $L = 8$. According to the suggested values in [25] and [27], we consider $L_b = 2$, $N_p = N/2 = 128$, $N_0 = 8$. For the sake of fairness, we present the number of CMs as a function of the required number of iteration, i_c, for iterative algorithms. However, in [25] and [27], $i_c = 120$ is suggested, while in our case, $i_c = 11$ is sufficient. Furthermore, table II presents the computational complexity of the receiver with different CFO synchronization techniques. As it is justified in section IX, in the case of 16-QAM modulation, we can consider $N_{\text{cor}} = 4$ and $i_p = 3$ for our iterative error correction in Algorithm 2. As it is shown, our proposed CFO estimation technique has lower computational complexity than other techniques except for the one proposed in [29]. However, it is demonstrated in section IX that our proposed technique provides a considerably higher performance as compared to the technique in [29].

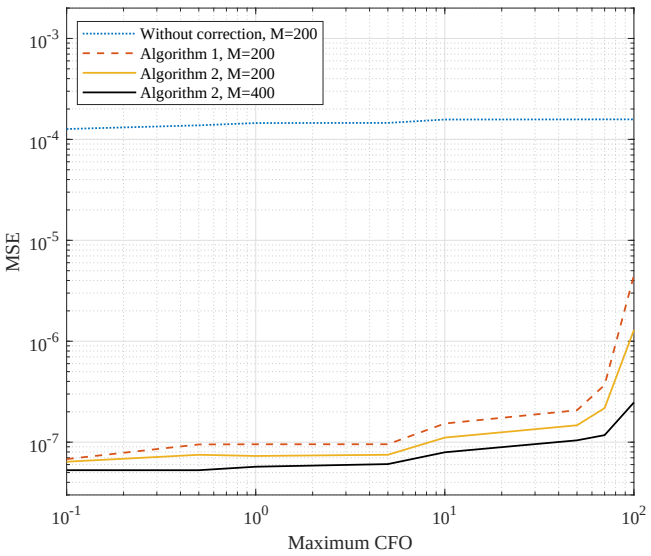

Figure 1. MSE of the proposed CFO estimation technique as a function of CFO for $N = 256$ subcarriers, 16-QAM modulation, and SNR$= -1$.

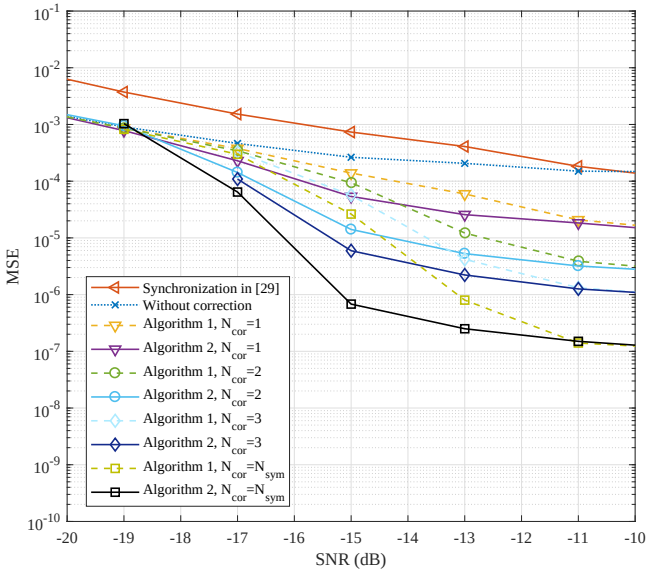

Figure 2. MSE of our proposed CFO estimation technique for $M = 200$ BS antennas, $P = 4$ users, $N = 256$ subcarriers, and 4-QAM modulation.

IX. Numerical Analysis

In this section, we confirm our theoretical developments in the previous sections through numerical simulations. We assume that $P = 4$ users are communicating over $N = 256$ subcarriers with a BS equipped with $M = 200$ antennas. In our simulations, we consider the 3GPP Long Term Evolution (LTE) channel model, extended typical urban (ETU) channel

Table I
COMPUTATIONAL COMPLEXITY OF THE DIFFERENT CFO ESTIMATION TECHNIQUES

Techniques	M=100	M=200	M=400
Proposed technique	$(0.2i_c + 6.5) \times 10^6$	$(0.2i_c + 13) \times 10^6$	$(0.2i_c + 26) \times 10^6$
Low-complexity [29], $\mathcal{C}_1^{\text{Est}}$	4.5×10^4	9×10^4	1.8×10^5
Constant-envelop pilot [30], $\mathcal{C}_2^{\text{Est}}$	4.2×10^8	8.3×10^8	1.7×10^9
Scattered pilot [25], $\mathcal{C}_3^{\text{Est}}$	$(20i_c + 0.4) \times 10^7$	$(10i_c + 0.2) \times 10^8$	$(7.3i_c + 0.1) \times 10^9$
Efficient Blind [27], $\mathcal{C}_4^{\text{Est}}$	$(0.6i_c + 4000) \times 10^7$	$(0.4i_c + 5000) \times 10^8$	$(0.3i_c + 5000) \times 10^9$

Table II
COMPUTATIONAL COMPLEXITY OF THE RECEIVER WITH DIFFERENT CFO SYNCHRONIZATION TECHNIQUES

Techniques	M=100	M=200	M=400
Proposed technique	$(0.2i_c + 26) \times 10^6$	$(0.2i_c + 53) \times 10^6$	$(0.2i_c + 100) \times 10^6$
Low-complexity [29]	2×10^7	4×10^7	8×10^7
Constant-envelop pilot [30]	4.4×10^8	9×10^8	1.8×10^9
Scattered pilot [25]	$(20i_c + 2.3) \times 10^7$	$(10i_c + 0.6) \times 10^8$	$(7.3i_c + 0.2) \times 10^9$
Efficient Blind [27]	$(0.6i_c + 4000) \times 10^7$	$(0.4i_c + 5000) \times 10^8$	$(0.3i_c + 5000) \times 10^9$

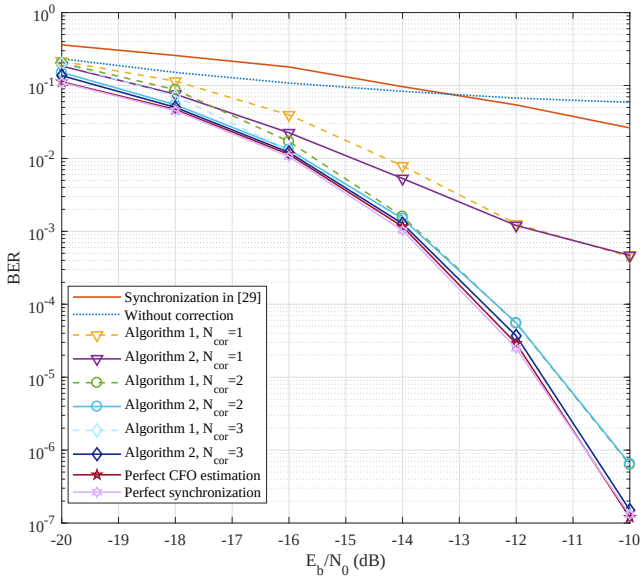

Figure 3. BER performance for $M = 200$ BS antennas, $P = 4$ users, $N = 256$ subcarriers, and 4-QAM modulation.

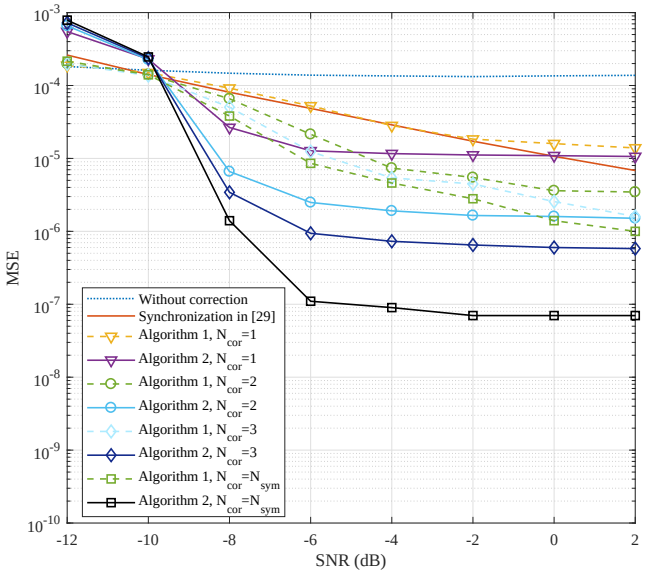

Figure 4. MSE of the proposed CFO estimation technique for $M = 200$ BS antennas, $P = 4$ users and $N = 256$ subcarriers with 16-QAM modulation.

model, [33], and the CP length of $N/8$. We assume perfect power control for all the users, 16-QAM modulation, and $N_{\text{sym}} = 10$ OFDM symbols in each data packet. In Fig. 1, we depict the MSE performance of our proposed estimation technique for different CFO ranges for SNR$= -1$. In order to obtain the curves in Fig. 1, the normalized CFO is randomly generated from a uniform distribution within the range $[-\epsilon_{\max}, \epsilon_{\max}]$, where $\epsilon_{\max}$ is the maximum CFO. It is shown that the performance of our proposed technique without correction is the same for all CFO values. Our results in Fig. 1 show that a substantial improvement can be achieved through application of our proposed error correction loop. Here, we have set $N_{\text{cor}} = N_{\text{sym}}$ and $\xi = 10^{-10}$. The MSE deterioration for large CFO values around 100 is due to the residual interference from noise and MUI, which can be reduced by deploying a larger number of BS antennas. Since the integer part of CFO can be estimated correctly and the error mainly comes from the fractional part of the CFO, we consider $\epsilon_{\max} = 0.5$ for the rest of our simulations.

In Fig. 2, the MSE performance of the system with 4-QAM modulation is depicted. As a comparison, we also plot the MSE of the CFO estimation method proposed in [29], which has the lowest computational complexity among other techniques. It is shown that while the performance of our proposed CFO estimation technique without error correction is close to the technique in [29], applying the estimation error

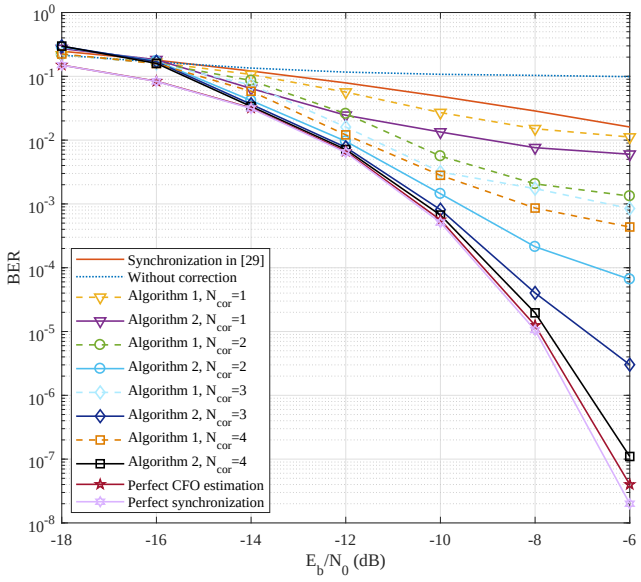

Figure 5. BER performance for $M = 200$ BS antennas, $P = 4$ users, $N = 256$ subcarriers and 16-QAM modulation.

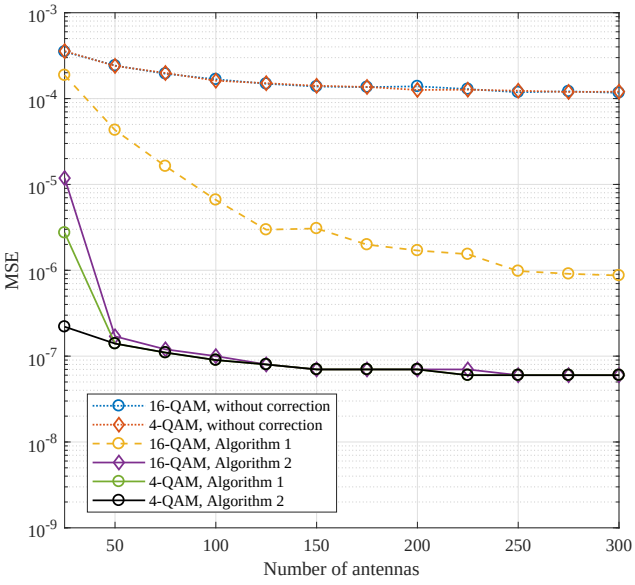

Figure 7. MSE of the proposed CFO estimation technique versus number of BS antennas for $SNR = -1$, $P = 4$ users and $N = 256$ subcarriers.

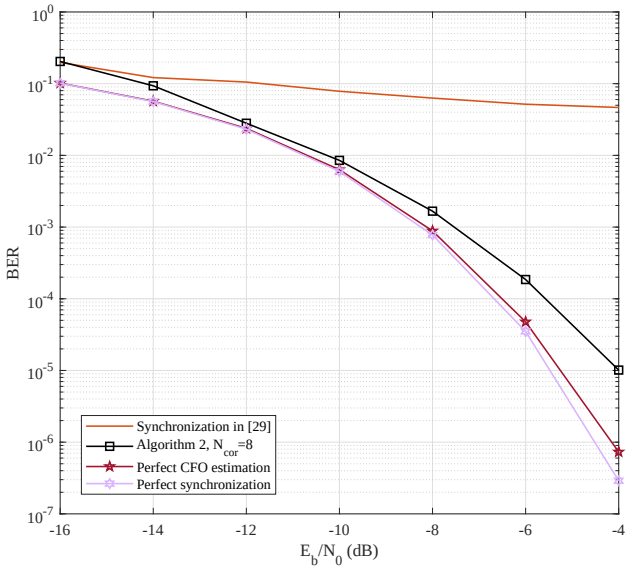

Figure 6. BER performance for $M = 200$ BS antennas, $P = 4$ users, $N = 256$ subcarriers and 64-QAM modulation.

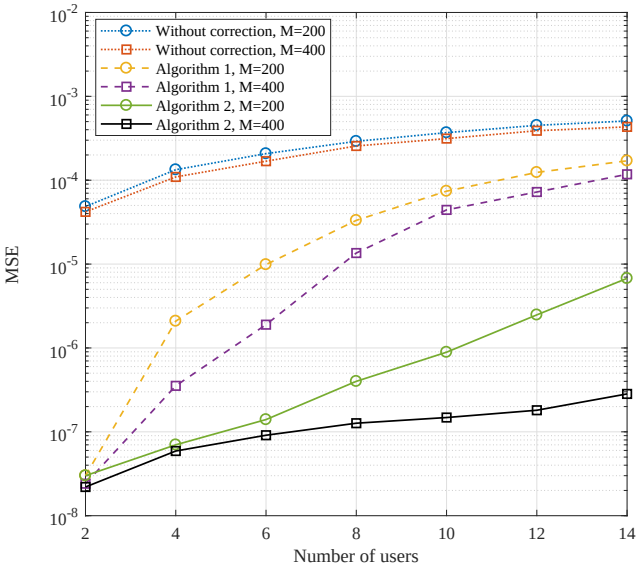

Figure 8. MSE of the proposed CFO estimation technique respect to number of users for $N = 256$ subcarriers, and $SNR = -1$.

correction algorithms lead to around three orders of magnitude improvement in the CFO estimation accuracy. Note that the error correction algorithm only corrects the phase shift error due to the CFO estimation error and does not change the CFO compensation matrix. Therefore, this performance improvement proves our claim that our proposed CFO compensation technique can effectively eliminate the scattering error and the phase shift is the only source of error. Note that this phase correction cannot enhance the performance of a system with the conventional CFO compensation, because the constellation of the received signal is scattered due to the CFO estimation error.

In Fig. 3, we demonstrate the BER performance of the system to evaluate our proposed CFO estimation and compensation techniques. Without loss of generality, our simulation results are obtained by transmission of raw data without application of any error correction coding technique. We compare our results with the perfect synchronization case as a benchmark. This figure shows that the BER performance is significantly improved through the proposed error correction algorithms, and for $N_{\text{cor}} = 3$ iterations, it almost matches the curve of the perfect CFO estimation, where $\tilde{\epsilon} = 0$.

The iterative correction in Algorithm 2 is more beneficial

for larger constellation sizes, where the constellation points are closer to one another. Thus, in order to highlight the difference between the two proposed algorithms, Fig. 4 presents the MSE performance for the system with 16-QAM modulation. As it is shown, the iterative correction in Algorithm 2 seems necessary to achieve an MSE of 10^{-7}. Note that according to equation (20), although the noise is negligible at higher SNRs, the MUI remains. Therefore, by taking into account the residual MUI, equation (28) can be updated as

$$\hat{\mathbf{d}}_q^{\kappa} = e^{-j\frac{2\pi}{N}\epsilon_q(N+N_{\mathrm{CP}})\kappa}\mathbf{\Omega}_{q,q}^{(-1)}(\mathbf{d}_q^{\kappa} + \sum_{\substack{p=0\\p\neq q}}^{P-1}\mathbf{\Omega}_{q,p}\mathbf{d}_p). \quad (59)$$

As the number of BS antennas grows large, the MUI term will be almost averaged out. It is worth noting that even a small amount of the residual MUI scatters the received signal constellation. This prevent us from achieving a perfect error calculation, and reflects as an error floor in the MSE curves. Furthermore, the BER performance of the system with 16-QAM modulation is studied in Fig. 5. As one can see, Algorithm 1 can improve the performance and outperform the technique in [29]. However, by increasing N_{cor} in the Algorithm 2, we can get the BER curve close to the perfect synchronization case. In addition, Fig 6 demonstrates the BER performance of the proposed synchronization technique for a large constellation size, i.e. 64-QAM. From Fig 6, one can realize that, the proposed synchronization technique is effective enough to work for large constellation sizes. However, the scattering effect of the residual MUI is more problematic than a smaller constellations, preventing us from achieving a perfect synchronization.

Furthermore, Fig. 7 shows how increasing the number of BS antennas can affect the MSE performance of our proposed CFO estimation technique. Regarding the proposed CFO estimation technique in Section III, a large number of BS antennas is required to have the noise terms efficiently averaged out and MUI diminished. As one can notice from Fig. 7, after a point where these requirements are fulfilled, no further enhancement can be achieved by increasing the number of BS antennas. On the other hand, the number of BS antennas should be large enough to provide an accurate equalization and CFO compensation, and separate the users' signals. Otherwise, the input signal to the error correction algorithms would be very scattered and lead to a poor phase shift error correction. The iterative error calculation in Algorithm 2 can deal with scattered data and provide the maximum MSE.

Finally, the MSE performance of our proposed CFO estimation technique with respect to the number of users is presented in Fig. 8. This figure demonstrates that our proposed synchronization technique can support a large number of users. In fact, since in massive MIMO systems, users share the whole available bandwidth, increasing the number of users affects the system performance as if the noise level is increased. As it is shown, larger number of BS antennas can average out the MUI and improve the performance.

X. Conclusion

In this paper, we proposed a new frequency synchronization technique for the uplink of multi-user OFDM-based massive MIMO systems. First, we proposed a CFO estimation technique whose complexity increases only linearly with respect to the number of BS antennas. Unlike the low-complexity technique proposed in [29], it does not require a long pilot. Second, we proposed a CFO compensation technique that takes place after combining the received signals at all the BS antennas. Consequently, its computational complexity is independent of the number of BS antennas. We also proved that after performing our CFO compensation technique, only a constant phase shift remains which is due to CFO estimation error. Then, we proposed an algorithm to efficiently calculate and remove this phase shift error. Numerical results were presented to verify the performance of our proposed synchronization technique. It was shown that the BER performance of our proposed technique is very close to that of a fully synchronous system. We also evaluated the CFO estimation accuracy and showed that MSE enhancement of 3 orders of magnitude can be achieved through application of our proposed error correction technique.

Acknowledgment

This publication has emanated from research conducted with the financial support of Science Foundation Ireland (SFI) and is co-funded under the European Regional Development Fund under Grant Number 13/RC/2077. Moreover, all calculations have performed on the CONNECT cluster maintained by the Trinity Centre for High Performance Computing.

Appendix

Proof of Unimodality of the Cost Function

The objective function of our optimization problem is the square of Frobenius norm of matrix $\check{\mathbf{\Lambda}}_q^{\perp}\mathbf{R}$ as it is shown in equation (7). By substituting this matrix from (5), we have

$$\left\|\check{\mathbf{\Lambda}}_q^{\perp}\mathbf{R}\right\|^2 = \left\|\hat{\mathbf{\Lambda}}_q^{\perp}\mathbf{\Lambda}_q\mathbf{C}_{q,q}\mathbf{\Lambda}_q^{\mathrm{H}} + \hat{\mathbf{\Lambda}}_q^{\perp}\mathbf{V}_q\right\|^2, \quad (60)$$

where the first term corresponds to the desired user q, and the second one is due to the noise plus multi-user interference with respect to user q. Equation (60) can be expanded as

$$\begin{aligned}\left\|\check{\mathbf{\Lambda}}_q^{\perp}\mathbf{R}\right\|^2 = \left\|\check{\mathbf{\Lambda}}_q^{\perp}\mathbf{\Lambda}_q\mathbf{W}_q\right\|^2 + \left\|\check{\mathbf{\Lambda}}_q^{\perp}\mathbf{V}_q\right\|^2 \\ + 2\Re\left\{\left\langle\check{\mathbf{\Lambda}}_q^{\perp}\mathbf{\Lambda}_q\mathbf{W}_q, \check{\mathbf{\Lambda}}_q^{\perp}\mathbf{V}_q\right\rangle\right\},\end{aligned} \quad (61)$$

where $\mathbf{W}_q = \mathbf{C}_{q,q}\mathbf{\Lambda}_q^{\mathrm{H}}$, $\check{\mathbf{\Lambda}}_q^{\perp} = \mathbf{P}_{X_q}\check{\mathbf{\Phi}}_q^{\mathrm{H}}$ for the trial CFO matrix $\check{\mathbf{\Phi}}_q$, and $\langle .,. \rangle$ is the Frobenius inner product. In the following, first we analyze these three terms separately, and then, we argue the unimodality of our objective function.

For the sake of simplicity and without loss of generality, we drop the index q from all of the vectors and matrices for the rest of this section. In addition, let us define $\mathbf{\Xi}_1 = \check{\mathbf{\Lambda}}^{\perp}\mathbf{\Lambda}\mathbf{W}$ and $\mathbf{\Xi}_2 = \check{\mathbf{\Lambda}}^{\perp}\mathbf{V}$, and rewrite the equation (61) as

$$\begin{aligned}\left\|\check{\mathbf{\Lambda}}^{\perp}\mathbf{R}\right\|^2 = \left\|\mathbf{\Xi}_1\right\|^2 + \left\|\mathbf{\Xi}_2\right\|^2 \\ + 2\Re\left\{\langle\mathbf{\Xi}_1, \mathbf{\Xi}_2\rangle\right\}.\end{aligned} \quad (62)$$

The first term of the right hand side of equation (62) can be calculated as

$$\left\|\boldsymbol{\Xi}_1\right\|^2 = \sum_{i=0}^{N-1}\sum_{j=0}^{N-1}\left|\Xi_1[i,j]\right|^2. \tag{63}$$

Then by defining $\mathbf{G} = \check{\boldsymbol{\Lambda}}^{\perp}\boldsymbol{\Lambda}$, we have

$$\begin{aligned}\left|\Xi_1[i,j]\right|^2 &= \left|\sum_{l=0}^{N-1} G[i,l]W[l,j]\right|^2 \\ &= \sum_{l=0}^{N-1}\sum_{k=0}^{N-1} G[i,l]W[l,j]G^*[i,k]W^*[k,j] \\ &= \sum_{l=0}^{N-1}\sum_{k=0}^{N-1} \left|G[i,l]\right|\left|G^*[i,k]\right| \mathrm{e}^{j(\angle G[i,l]-\angle G[i,k])} \\ &\quad\times \left|W[l,j]\right|\left|W^*[k,j]\right| \mathrm{e}^{j(\angle W[i,l]-\angle W[i,k])}. \end{aligned}\tag{64}$$

The elements of the matrix $\mathbf{W}$ are independent of the trial CFO values, and the ij^{th} entry of $\mathbf{G}$ is given by

$$\begin{aligned} G[i,j] &= \sum_{l=0}^{N-1} P_X[i,l]\check{\Phi}^*[l,l]\Phi[l,l]X[l,j] \\ &= \sum_{l=0}^{N-1} P_X[i,l]\tilde{\Phi}^*[l,l]X[l,j] \\ &= \left\langle \tilde{\boldsymbol{\lambda}}_i^{\perp}, \mathbf{x}_j \right\rangle \\ &= \left\|\tilde{\boldsymbol{\lambda}}_i^{\perp}\right\| \left\|\mathbf{x}_j\right\| \cos(\theta_{\mathrm{C}}(\tilde{\boldsymbol{\lambda}}_i^{\perp}, \mathbf{x}_j)), \end{aligned}\tag{65}$$

for $0 \le i,j \le N-1$ where $\tilde{\Phi}[l,l] = e^{j\frac{2\pi}{N}\tilde{\epsilon}(l+N_{\mathrm{CP}})}$, and $\tilde{\epsilon}$ is the difference between the desired CFO, ϵ, and the trial CFO value, $\check{\epsilon}$. In addition, $\tilde{\boldsymbol{\lambda}}_i^{\perp}$ is the i^{th} row of the matrix $\tilde{\boldsymbol{\Lambda}}^{\perp} = \mathbf{P}_X\tilde{\boldsymbol{\Phi}}^{\mathrm{H}}$, $\mathbf{x}_j$ is the j^{th} column of the matrix $\mathbf{X}$, and $\theta_{\mathrm{C}}(\tilde{\boldsymbol{\lambda}}_i^{\perp}, \mathbf{x}_j)$ is the angle between the two complex vectors $\tilde{\boldsymbol{\lambda}}_i^{\perp}$ and $\mathbf{x}_j$. Since $\mathbf{P}_X$ is defined to be the orthogonal projection onto the space spanned by the columns of the matrix $\mathbf{X}$, the i^{th} row of the matrix $\mathbf{P}_X$, and the vector $\mathbf{x}_j$ are orthogonal for any $i,j \in [0, N-1]$. Hence, if $\check{\epsilon} = \epsilon$, $\tilde{\boldsymbol{\Phi}} = \mathbf{I}_N$ and we have

$$\left\langle \tilde{\boldsymbol{\lambda}}_i^{\perp}, \mathbf{x}_j \right\rangle = 0, \tag{66}$$

this means $\cos(\theta_{\mathrm{C}}(\tilde{\boldsymbol{\lambda}}_i^{\perp}, \mathbf{x}_j)) = 0$ and $\theta_{\mathrm{C}}(\tilde{\boldsymbol{\lambda}}_i^{\perp}, \mathbf{x}_j) = \pm\pi/2$ for any i and j. Thus, $\mathbf{G}$ becomes a zero matrix, and $\left\|\boldsymbol{\Xi}_1\right\|^2 = 0$.

If $\check{\epsilon} \neq \epsilon$ the orthogonality between the two vectors $\tilde{\boldsymbol{\lambda}}_i^{\perp}$ and $\mathbf{x}_j$ is destroyed. Consider the singular value decomposition (SVD) of the matrix $\mathbf{P}_X$ as $\mathbf{P}_X = \mathbf{U}\boldsymbol{\Sigma}\mathbf{V}^{\mathrm{H}}$. Then, by multiplying $\mathbf{P}_X$ to $\tilde{\boldsymbol{\Phi}}$, the right singular vectors of the matrix $\mathbf{P}_X$, i.e. the columns of $\mathbf{V}$, are multiplied to the matrix $\tilde{\boldsymbol{\Phi}}$. This means that the orthogonal basis of the matrix $\mathbf{P}_X$ are rotated by $\tilde{\epsilon}$, which is the difference between the desired CFO, ϵ, and the trial CFO, $\check{\epsilon}$. Therefore, the resulting matrix is not orthogonal to $\mathbf{X}$ anymore, and the length of the projection of $\tilde{\boldsymbol{\lambda}}_i^{\perp}$ on $\mathbf{x}_j$, i.e. $\left\langle \tilde{\boldsymbol{\lambda}}_i^{\perp}, \mathbf{x}_j \right\rangle$, is a function of $\tilde{\epsilon}$. Note that $\cos(\theta_{\mathrm{C}}(\mathbf{a},\mathbf{b}))$ has a complex value which can be represented as

$$\cos(\theta_C(\mathbf{a},\mathbf{b})) = \gamma \mathrm{e}^{i\varphi}, \tag{67}$$

where

$$\gamma = \cos(\theta_{\mathrm{H}}(\mathbf{a},\mathbf{b})) = |\cos(\theta_{\mathrm{C}}(\mathbf{a},\mathbf{b}))|, \tag{68}$$

$0 \le \theta_{\mathrm{H}} \le \pi/2$ is called the Hermitian angle between the vectors $\mathbf{a}$ and $\mathbf{b}$ of the complex vector space, and $-\pi \le \varphi \le \pi$ is called their (Kasner's) pseudo-angle [34]. Since $\theta_{\mathrm{C}}(\tilde{\boldsymbol{\lambda}}_i^{\perp}, \mathbf{x}_j) = \pm\pi/2$ for $\tilde{\epsilon} = 0$, any rotation less than $\pi/2$ will increase the value of $\cos(\theta_{\mathrm{H}}(\tilde{\boldsymbol{\lambda}}_i^{\perp}, \mathbf{x}_j)) = |\cos(\theta_{\mathrm{C}}(\tilde{\boldsymbol{\lambda}}_i^{\perp}, \mathbf{x}_j))|$, and hence the larger the rotation, the larger the value of $\cos(\theta_{\mathrm{H}}(\tilde{\boldsymbol{\lambda}}_i^{\perp}, \mathbf{x}_j))$. If $|\tilde{\epsilon}| < 1$, the rotation cannot be greater than $\pi/2$. Therefore, as $|\tilde{\epsilon}|$ grows, the absolute value of the elements in the matrix $\mathbf{G}$ increase.

Moreover, since all the orthogonal basis vectors of the matrix $\mathbf{P}_X$ are rotated by the value of $\tilde{\epsilon}$, $\theta_{\mathrm{C}}(\tilde{\boldsymbol{\lambda}}_i^{\perp}, \mathbf{x}_j)$ is the same for every $i,j \in [0, N-1]$. Hence, considering $\angle G[i,j] = \angle\cos(\theta_{\mathrm{C}}(\tilde{\boldsymbol{\lambda}}_i^{\perp}, \mathbf{x}_j))$, $\angle G[i,l] = \angle G[i,k]$ for any amount of $\tilde{\epsilon}$, and we have

$$\begin{aligned}\left|\Xi_1[i,j]\right|^2 &= \sum_{l=0}^{N-1}\left|G[i,l]\right|^2\left|W[l,j]\right|^2 \\ &\quad + 2\sum_{l=0}^{N-2}\sum_{k=l+1}^{N-1}\left|G[i,l]\right|\left|G^*[i,k]\right| \\ &\quad\times \left|W[l,j]\right|\left|W^*[k,j]\right|\cos(\angle W[i,l]-\angle W[i,k])). \end{aligned}\tag{69}$$

Then, because $|G[i,j]|$ increases as $|\tilde{\epsilon}|$ grows, $\left|\Xi_1[i,j]\right|^2$ will also increase. Hence, if $|\check{\epsilon_2}-\epsilon| > |\check{\epsilon_1}-\epsilon|$, we have $\left\|\boldsymbol{\Xi}_1\right\|^2|_{\check{\epsilon_2}} > \left\|\boldsymbol{\Xi}_1\right\|^2|_{\check{\epsilon_1}}$ for any $\check{\epsilon}$, and $\left\|\boldsymbol{\Xi}_1\right\|^2 = 0$ for $\check{\epsilon} = \epsilon$. As a result, the first term of the right hand side of equation (62) is a unimodal function with respect to the trial CFO value.

The second term of the right hand side of equation (62) can be calculated as

$$\left\|\boldsymbol{\Xi}_2\right\|^2 = \sum_{i=0}^{N-1}\sum_{j=0}^{N-1}\left|\Xi_2[i,j]\right|^2, \tag{70}$$

where

$$\begin{aligned}\left|\Xi_2[i,j]\right|^2 &= \left|\sum_{l=0}^{N-1}\check{\Lambda}^{\perp}[i,l]V[l,j]\right|^2 \\ &= \sum_{l=0}^{N-1}\sum_{k=0}^{N-1}\check{\Lambda}^{\perp}[i,l]V[l,j](\check{\Lambda}^{\perp})^*[i,k]V^*[k,j]. \end{aligned}\tag{71}$$

Then, by substituting $\check{\boldsymbol{\Lambda}}^{\perp} = \mathbf{P}_X\check{\boldsymbol{\Phi}}^{\mathrm{H}}$ in equation (71), we have

$$\begin{aligned}\left|\Xi_2[i,j]\right|^2 &= \sum_{l=0}^{N-1}\sum_{k=0}^{N-1} P_X[i,l]P_X^*[i,k] \\ &\quad\times V[l,j]V^*[k,j]\mathrm{e}^{j\frac{2\pi}{N}\check{\epsilon}(k-l)}. \end{aligned}\tag{72}$$

By substituting (72) in (70), $\left\|\boldsymbol{\Xi}_2\right\|^2$ is given by

$$\left\|\boldsymbol{\Xi}_2\right\|^2 = \zeta + \sum_{l=0}^{N-1}\sum_{\substack{k=0\\k\neq l}}^{N-1} T[l,k]\mathrm{e}^{j\frac{2\pi}{N}\check{\epsilon}(k-l)}, \tag{73}$$

where

$$\zeta = \sum_{i=0}^{N-1}\sum_{j=0}^{N-1}\sum_{l=0}^{N-1} |P_X[i,l]|^2 \, |V[l,j]|^2 , \tag{74}$$

and

$$T[l,k] = \sum_{i=0}^{N-1} P_X[i,l] P_X^*[i,k] \sum_{j=0}^{N-1} V[l,j] V^*[k,j]. \tag{75}$$

Note that ζ is constant with respect to $\check{\epsilon}$. Moreover, since $T[l,k] = T^*[k,l]$, $\|\boldsymbol{\Xi}_2\|^2$ can be rewritten as

$$\|\boldsymbol{\Xi}_2\|^2 = \zeta + 2\sum_{l=0}^{N-2}\sum_{\substack{k=l+1 \\ k\neq l}}^{N-1} |T[l,k]| \times \cos(\angle T[l,k] + \frac{2\pi}{N}\check{\epsilon}(k-l)). \tag{76}$$

The second term in equation (76) is a sum of $N(N-1)/2$ number of cosine functions of $\check{\epsilon}$ with different periods in the range of $1 < N/(k-l) \leq N$. Thus, the value of these cosine functions vary slowly. In addition, since $l \neq k$ for $T[l,k]$ in equation (73), the elements of the matrices $\mathbf{P}_X$ and $\mathbf{V}$ in equation (75) are statistically independent. Consequently, the elements $T[l,k]$ are very small and tend to zero. Thus, the second term in the right hand side of equation (62) can be approximated to a constant value with respect to the trial CFO.

Finally, considering the third term in the right hand side of equation (62), we have

$$\Re\{\langle \boldsymbol{\Xi}_1, \boldsymbol{\Xi}_2 \rangle\} = \sum_{i=0}^{N-1}\sum_{j=0}^{N-1} |\Xi_1[i,j]| \, |\Xi_2[i,j]| \cos(\theta_\Xi), \tag{77}$$

where $\theta_\Xi = \angle\Xi_2[i,j] - \angle\Xi_1[i,j]$. Following similar line of derivations as above, it can be shown that $|\Xi_1[i,j]|$ is also unimodal with respect to the trial CFO values, and $|\Xi_2[i,j]|$ remains constant as $\check{\epsilon}$ changes. Since $|\Xi_2[i,j]|$ is always positive, $|\Xi_1[i,j]| \, |\Xi_2[i,j]|$ is just a scaled version of $|\Xi_1[i,j]|$ which is unimodal with the same minimum point as $|\Xi_1[i,j]|$ for any $i,j \in [0, N-1]$. Then, for given i and j, if $\cos(\theta_\Xi) > 0$, it only multiplies to the scale of $|\Xi_1[i,j]|$. Else if $\cos(\theta_\Xi) < 0$, beside changing the scale, it also turns it to a downward unimodal function.

In addition, since adding a constant value does not disturb the unimodality, the sum of the first two terms in equation (62) is an upward unimodal function that gets its minimum at the trial CFO value that minimize $|\Xi_1[i,j]|$. Therefore, as long as the value of the third term is smaller than the sum of the two first terms for any i,j, and $\check{\epsilon}$, the overall cost function in (62) will be an upward unimodal function. To this end, the following inequality should be fulfilled for any i and j value.

$$|\Xi_1[i,j]|^2 + |\Xi_2[i,j]|^2 > |\Xi_1[i,j]| \, |\Xi_2[i,j]| \cos(\theta_\Xi). \tag{78}$$

Since $\cos(\theta_\Xi) \in [-1, 1]$, the sufficient condition to guarantee unimodality is

$$|\Xi_1[i,j]|^2 + |\Xi_2[i,j]|^2 > |\Xi_1[i,j]| \, |\Xi_2[i,j]| . \tag{79}$$

We know that the inequality

$$(|\Xi_1[i,j]| - |\Xi_2[i,j]|)^2 > 0, \tag{80}$$

is always true. Hence,

$$|\Xi_1[i,j]|^2 + |\Xi_2[i,j]|^2 > 2\,|\Xi_1[i,j]| \, |\Xi_2[i,j]| > |\Xi_1[i,j]| \, |\Xi_2[i,j]| , \tag{81}$$

is also true, and the sufficient condition for unimodality is fulfilled. Therefore, even when $\cos(\theta_\Xi) < 0$, the final expression of the cost function for given i and j values is an upward unimodal function with respect to the trial CFO values.

As a conclusion, we have proved that the first term on the right hand side of the equation (62) is unimodal, the second term is constant which means the sum of the first two terms is also unimodal. Moreover, it is argued that for any i,j and ϵ, the third term of this equation preserves the unimodality of the whole objective function. Therefore, our objective function is an upward unimodal and its minimum can be found using search algorithms such as Golden section search.

REFERENCES

[1] P. Sabeti, A. Farhang, N. Marchetti, and L. Doyle, "Low-complexity CFO compensation for OFDM-based massive MIMO systems," in *IEEE Globecom Workshops (GC Wkshps)*, 2017, pp. 1–7.

[2] J. G. Andrews, S. Buzzi, W. Choi, S. V. Hanly, A. Lozano, A. C. Soong, and J. C. Zhang, "What will 5G be?" *IEEE Journal on Selected Areas in Communications*, vol. 32, no. 6, pp. 1065–1082, 2014.

[3] E. G. Larsson, O. Edfors, F. Tufvesson, and T. L. Marzetta, "Massive MIMO for next generation wireless systems," *IEEE Communications Magazine*, vol. 52, no. 2, pp. 186–195, 2014.

[4] F. Rusek, D. Persson, B. K. Lau, E. G. Larsson, T. L. Marzetta, O. Edfors, and F. Tufvesson, "Scaling up MIMO: Opportunities and challenges with very large arrays," *IEEE Signal Processing Magazine*, vol. 30, no. 1, pp. 40–60, 2013.

[5] T. L. Marzetta, "Noncooperative cellular wireless with unlimited numbers of base station antennas," *IEEE Transactions on Wireless Communications*, vol. 9, no. 11, pp. 3590–3600, 2010.

[6] E. Björnson, J. Hoydis, and L. Sanguinetti, "Massive MIMO has unlimited capacity," *IEEE Transactions on Wireless Communications*, vol. 17, no. 1, pp. 574–590, 2018.

[7] H. Q. Ngo, E. G. Larsson, and T. L. Marzetta, "Energy and spectral efficiency of very large multiuser MIMO systems," *IEEE Transactions on Communications*, vol. 61, no. 4, pp. 1436–1449, 2013.

[8] J. G. Andrews, T. Bai, M. N. Kulkarni, A. Alkhateeb, A. K. Gupta, and R. W. Heath, "Modeling and analyzing millimeter wave cellular systems," *IEEE Transactions on Communications*, vol. 65, no. 1, pp. 403–430, 2017.

[9] M. Ganji and H. Jafarkhani, "On the performance of MRC receiver with unknown timing mismatch-a large scale analysis," *arXiv preprint arXiv:1703.10422*, 2017.

[10] V. Kotzsch and G. Fettweis, "Interference analysis in time and frequency asynchronous network MIMO OFDM systems," in *IEEE Wireless Communications and Networking Conference (WCNC)*, 2010, pp. 1–6.

[11] C. Shan, Y. Zhang, L. Chen, X. Chen, and W. Wang, "Performance analysis of large scale antenna system with carrier frequency offset, quasi-static mismatch and channel estimation error," *IEEE Access*, vol. 5, pp. 26 135–26 145, 2017.

[12] K. Raghunath and A. Chockalingam, "SIR analysis and interference cancellation in uplink OFDMA with large carrier frequency/timing offsets," *IEEE Transactions on Wireless Communications*, vol. 8, no. 5, 2009.

[13] T. M. Schmidl and D. C. Cox, "Robust frequency and timing synchronization for OFDM," *IEEE transactions on communications*, vol. 45, no. 12, pp. 1613–1621, 1997.

[14] A. Farhang, N. Marchetti, L. E. Doyle, and B. Farhang-Boroujeny, "Low complexity CFO compensation in uplink OFDMA systems with receiver windowing." *IEEE Transactions on Signal Processing*, vol. 63, no. 10, pp. 2546–2558, 2015.

[15] H. Minn, V. K. Bhargava, and K. B. Letaief, "A robust timing and frequency synchronization for OFDM systems," *IEEE Transactions on Wireless Communications*, vol. 2, no. 4, pp. 822–839, 2003.

[16] J. Chen, Y.-C. Wu, S. Ma, and T.-S. Ng, "Joint CFO and channel estimation for multiuser MIMO-OFDM systems with optimal training sequences," *IEEE transactions on signal processing*, vol. 56, no. 8, pp. 4008–4019, 2008.

[17] Y. Wu, J. W. Bergmans, and S. Attallah, "Carrier frequency offset estimation for multiuser MIMO OFDM uplink using CAZAC sequences: performance and sequence optimization," *EURASIP Journal on Wireless Communications and Networking*, vol. 2011, no. 1, p. 570680, 2011.

[18] Y.-R. Tsai, H.-Y. Huang, Y.-C. Chen, and K.-J. Yang, "Simultaneous multiple carrier frequency offsets estimation for coordinated multi-point transmission in OFDM systems," *IEEE transactions on wireless communications*, vol. 12, no. 9, pp. 4558–4568, 2013.

[19] V. Kotzsch, J. Holfeld, and G. Fettweis, "Joint detection and CFO compensation in asynchronous multi-user MIMO OFDM systems," in *IEEE Vehicular Technology Conference (VTC)*, 2009, pp. 1–5.

[20] H. Huang, W. G. Wang, and J. He, "Phase noise and frequency offset compensation in high frequency MIMO-OFDM system," in *IEEE International Conference on Communications (ICC)*, 2015, pp. 1280–1285.

[21] H. V. Cheng and E. G. Larsson, "Some fundamental limits on frequency synchronization in massive MIMO," in *IEEE Asilomar Conference on Signals, Systems and Computers*, 2013, pp. 1213–1217.

[22] H. Hojatian, M. J. Omidi, H. Saeedi-Sourck, and A. Farhang, "Joint CFO and channel estimation in OFDM-based massive MIMO systems," in *IEEE International Symposium on Telecommunications (IST)*, 2016, pp. 343–348.

[23] W. Zhang, F. Gao, and H.-M. Wang, "Frequency synchronization for massive MIMO multi-user uplink," in *IEEE Global Communications Conference (GLOBECOM)*, 2016, pp. 1–6.

[24] W. Zhang, F. Gao, S. Jin, and H. Lin, "Frequency synchronization for uplink massive MIMO systems," *IEEE Transactions on Wireless Communications*, vol. 17, no. 1, pp. 235–249, 2018.

[25] W. Zhang, F. Gao, H. Minn, and H.-M. Wang, "Scattered pilots-based frequency synchronization for multiuser OFDM systems with large number of receive antennas," *IEEE Transactions on Communications*, vol. 65, no. 4, pp. 1733–1745, 2017.

[26] W. Zhang and F. Gao, "Blind frequency synchronization for multiuser OFDM uplink with large number of receive antennas," *IEEE Transactions on Signal Processing*, vol. 64, no. 9, pp. 2255–2268.

[27] Y. Feng, W. Zhang, F. Gao, and Q. Sun, "Computationally efficient blind CFO estimation for massive MIMO uplink," *IEEE Transactions on Vehicular Technology*, 2018.

[28] W. Zhang, Q. Yin, and F. Gao, "Computationally efficient blind estimation of carrier frequency offset for MIMO-OFDM systems," *IEEE Transactions on Wireless Communications*, vol. 15, no. 11, pp. 7644–7656, 2016.

[29] S. Mukherjee and S. K. Mohammed, "Low-complexity CFO estimation for multi-user massive MIMO systems," in *IEEE Global Communications Conference (GLOBECOM)*, 2015, pp. 1–7.

[30] S. Mukherjee, S. K. Mohammed, and I. Bhushan, "Impact of CFO estimation on the performance of ZF receiver in massive MU-MIMO systems," *IEEE Transactions on Vehicular Technology*, vol. 65, no. 11, pp. 9430–9436, 2016.

[31] W. H. Press, S. A. Teukolsky, W. T. Vetterling, and B. P. Flannery, "Golden section search in one dimension," *Numerical Recipies in C: the Art of Scientific Computing*, vol. 2, 1992.

[32] G. Strang, *Introduction to linear algebra*. Wellesley-Cambridge Press Wellesley, MA, 1993, vol. 3.

[33] W.-B. Yang and M. Souryal, *LTE physical layer performance analysis*. US Department of Commerce, National Institute of Standards and Technology, 2014.

[34] K. Scharnhorst, "Angles in complex vector spaces," *Acta Applicandae Mathematica*, vol. 69, no. 1, pp. 95–103, 2001.

Parna Sabeti received the B.Sc. degree in electronic engineering from Shiraz University of Technology, Shiraz, Iran, in 2012, and the M.Sc. degree in telecommunications engineering from Isfahan University of Technology, Isfahan, Iran, in 2015. She is currently working toward the Ph.D. degree at the Irish National Telecommunications Research Centre (CONNECT), Trinity College Dublin, Ireland. Her research interests include signal processing, wireless communications, machine learning, multi-antenna and multicarrier systems.

Arman Farhang received the B.Sc. degree in telecommunications engineering from the Islamic Azad University, Najafabad, Iran, in 2007, the M.Sc. degree in telecommunications engineering from the Sadjad University of Technology, Mashhad, Iran, in 2010, and the Ph.D. degree from the Trinity College Dublin, Dublin, Ireland, in 2016. Since then, he was a Research Fellow with the Irish National Telecommunications Research Centre (CONNECT), Trinity College Dublin, Ireland until 2018. He served as a Lecturer with the School of Electrical and Electronic Engineering, University College Dublin, Ireland during the year 2018. He joined the Department of Electronic Engineering at Maynooth University in September 2018 where he currently holds a lecturer position. Dr Farhang is an associated investigator in the CONNECT centre where he leads the research around the topic of waveforms for 5G and beyond. His areas of research include wireless communications, digital signal processing for communications, multiuser communications, multiantenna and multicarrier systems.

Nicola Marchetti received the M.Sc. degree in electronic engineering from the University of Ferrara, Italy, in 2003, and the Ph.D. degree in wireless communications in 2007. He also received the M.Sc. degree in mathematics, in 2010, both from Aalborg University, Denmark. He is currently an Assistant Professor at Trinity College Dublin, Ireland, and is a member of CONNECT Research Centre. His collaborations to date include research projects in cooperation with Samsung, Nokia Bell Labs, Intel Mobile Communications, among others. His research interests include: Complex Systems Science, Radio Resource Management, Self-Organizing Networks, and Signal Processing.

Linda Doyle Prof. Doyle is the VP of Research /Dean of Research and Professor of Engineering and The Arts in Trinity College, University of Dublin. She was the founder Director of CONNECT a national research centre, co-funded by SFI and industry, focused on future networks and communications. Prior to CONNECT Prof. Doyle was also the Director of CTVR. Her expertise is in the fields of wireless communications, cognitive radio, reconfigurable networks, spectrum management and creative arts practices. Prof. Doyle has a reputation as an advocate for change in spectrum management practices and has played a role in spectrum policy at the national and international level. Currently she is a member of the National Broadband Steering Committee in Ireland, and is Chair of the Ofcom Spectrum Advisory Board in the UK. She is a Fellow of Trinity College Dublin. She is on the Board of the Festival of Curiosity A STEM outreach activity for children based on a city-centre yearly science festival. She is a judge in the BT Young Scientist, Ireland's premier science competition for school children. She is the Chair of the Board of the Douglas Hyde Gallery and sits on the Board of Pallas Project Studios. Prof. Doyle is a Director of Xcelerit and SRS, two CTVR/CONNECT spin-outs.